Inorganic Chemistry

Article

pubs.acs.org/IC

Incorporation of Amphiphilic Ruthenium(II) Ammine Complexes into Langmuir–Blodgett Thin Films with Switchable Quadratic Nonlinear Optical Behavior

Leïla Boubekeur-Lecaque,[†] Benjamin J. Coe,*[,†] James A. Harris,[†] Madeleine Helliwell,[†] Inge Asselberghs,[‡] Koen Clays,[‡] Stijn Foerier,[‡] and Thierry Verbiest[‡]

[†]School of Chemistry, University of Manchester, Oxford Road, Manchester M13 9PL, U.K.

[‡]Department of Chemistry, University of Leuven, Celestijnenlaan 200D, B-3001 Leuven, Belgium

Supporting Information

ABSTRACT: Nine nonlinear optical (NLO) chromophores with pyridinium electron acceptors have been synthesized by complexing new proligands with $\{Ru^{II}(NH_3)_5\}^{2+}$ electron-donor centers. The presence of long alkyl/fluoroalkyl chain substituents imparts amphiphilic properties, and these cationic complexes have been characterized as their PF_6^- salts by using various techniques including electronic absorption spectroscopy and cyclic voltammetry. Each complex shows three reversible/quasireversible redox processes; a $Ru^{III/II}$ oxidation and two ligand-based reductions. The energies of the intense visible d → π* metal-to-ligand charge-transfer (MLCT) absorptions correlate to some extent with the ligand reduction potentials. ^1H NMR spectroscopy also provides insights into the relative electron-withdrawing strengths of the new ligands. Single crystal X-ray structures have been determined for two of the proligand salts and one complex salt, $[Ru^{II}(NH_3)_5(4\text{-}C_{16}H_{33}PhQ^+)]Cl_3\cdot 3.25H_2O$ (PhQ^+ = *N*-phenyl-4,4′-bipyridinium), showing centrosymmetric packing structures in each case. The PF_6^- analogue of the latter complex has been used to deposit reproducibly high-quality, multilayered Langmuir–Blodgett (LB) thin films. These films show a strong second harmonic generation (SHG) response from a 1064 nm laser; their MLCT absorbance increases linearly with the number of layers (*N*) and $I_{2\omega}/I_{\omega}^2$ ($I_{2\omega}$ = intensity at 532 nm; I_{ω} = intensity at 1064 nm) scales quadratically with *N*, consistent with homogeneous deposition. LB films on indium tin oxide (ITO)-coated glass show electrochemically induced switching of the SHG response, with a decrease in activity of about 50% on $Ru^{II} \rightarrow Ru^{III}$ oxidation. This effect is reversible, but reproducible over only a few cycles before the signal from the Ru^{II} species diminishes. This work extrapolates our original solution studies (Coe, B. J. et al. *Angew. Chem., Int. Ed.* **1999**, *38*, 366) to the first demonstration of redox-switching of NLO activity in a molecular material.

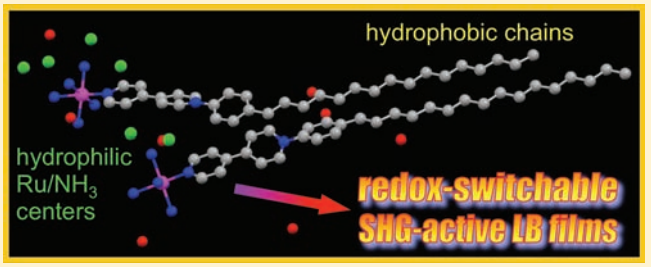

INTRODUCTION

The promise of diverse applications including optical data processing and biological imaging has stimulated much interest in organic nonlinear optical (NLO) materials.[1] Within this field, organotransition metal complexes offer intriguing possibilities for the creation of new multifunctional materials in which potentially useful optical behavior is combined with redox, magnetic, and other properties that are characteristic of such compounds.[2] As a means to enhance the prospects for molecular materials, approaches to the reversible modulation of molecular NLO properties have attracted considerable attention over recent years.[3] The first report of a very pronounced and reversible redox-switching of the first hyperpolarizability β (the origin of quadratic molecular NLO effects) provides a clear demonstration of the potential significance of metal complexes in this area.[4] Various related solution and molecular-level theoretical studies involving both quadratic and cubic NLO effects have been described since,[5] but very little corresponding work with more organized materials has appeared and none with well-understood systems. Kondo et al. reported redox-switching of second harmonic generation (SHG) from self-assembled monolayers (SAMs) of ferrocenyl-thiols on gold electrodes.[6] However, these SAMs greatly decrease the 532 nm SHG intensity when compared with that from bare gold and a 4–6-fold intensity increase was, counterintuitively, ascribed to oxidation of the ferrocenyl electron donor groups. This claim was supported by increased β responses for the oxidized species derived from ZINDO calculations. Subsequent independent studies have confirmed that oxidizing ferrocenyl units decreases β,[5b] so it is likely that the effects observed by Kondo et al. arise solely from changes in the orientation of the molecules within the SAM (originally claimed to be merely a contributing factor).[6]

To make the next step toward potential applications of switchable NLO phenomena, a number of significant challenges

Received: October 4, 2011
Published: November 11, 2011

must be overcome, especially for quadratic effects that have crucial symmetry requirements. First, it is necessary to incorporate active chromophores into polar bulk materials, with very large numbers of molecules required to give significant and potentially useful effects. Second, the material must be readily addressable by an external stimulus; for electrochemical and most optical device purposes thin films are required. Long-term thermal and optical stability are further key requirements for any real-world applications.

We have studied many dipolar Ru^{II} ammine complexes which show low energy metal-to-ligand charge-transfer (MLCT) transitions associated with very large static first hyperpolarizabilities β_0.[7] The optical properties of such chromophores are especially well understood and ideally suited to external control.[4] Noncentrosymmetric arrangements of NLO chromophores can be created on various substrates by using the Langmuir−Blodgett (LB) deposition technique,[8] and several reports of Ru^{II} complexes showing NLO effects in LB films have appeared.[9] For example, an early study noted SHG from a nitrile complex of $\{Ru^{II}(\eta^5\text{-}C_5H_5)(PPh_3)_2\}^+$,[9a] and a small photoinduced modulation of SHG at 295 nm from alternating and highly diluted films containing a derivative of $[Ru^{II}(2,2'\text{-bpy})_3]^{2+}$ (bpy = bipyridyl) was attributed to changes in β on MLCT excitation.[9b] However, the ground state complex shows an intense bpy-based absorption near the SHG wavelength, so excitation-induced changes in absorption may affect the SHG signal. Sortino, Di Bella, and co-workers have recently reported redox-switching of linear optical absorption in SAMs of $\{Ru^{II}(NH_3)_5\}^{2+}$-4,4′-bipyridinium complexes on transparent platinum electrodes,[10] and have also described Langmuir-Schäfer (LS) films of salt **1**.[11] In other related studies, SAMs of a $[Ru^{II}(2,2'\text{-bpy})_3]^{2+}$ derivative on indium tin oxide (ITO) have shown redox-switching of the UV absorption because of a ligand-based $\pi \rightarrow \pi^*$ transition.[12] Although SAMs are inherently noncentrosymmetric, the fact that they are only one molecule thick means that the observation of significant NLO effects would require an extremely active chromophore. The present report describes the formation of high quality LB multilayers containing the Ru^{II} ammine complex salt **5** that display large, switchable SHG signals. Some of the results described herein have been communicated previously.[13]

EXPERIMENTAL SECTION

Materials and Procedures. All reactions were performed under an Ar atmosphere and in Ar-purged solvents. The compounds $[Ru^{II}(NH_3)(H_2O)][PF_6]_2$,[14] 4-aminobenzoic acid *n*-hexadecylester,[15] 4-amino-*N*-*n*-hexadecyl-*N*-methyl-benzenesulfonamide,[16] and *N*-(2,4-dinitrophenyl)-4,4′-bipyridinium chloride ([2,4-DNPhQ$^+$]-Cl·0.5EtOH·0.25H_2O)[17] were synthesized by following previously published methods. The compound 4-(perfluoro-*n*-octylthio)aniline has been reported previously,[18] but we were unable to obtain satisfactory results by using the published procedure, so developed a modified approach. All other reagents were obtained commercially and used as supplied. Products were dried overnight in a vacuum desiccator ($CaSO_4$) prior to any characterization and were heated under vacuum at about 100 °C before CHN analyses.

General Physical Measurements. ^{1}H NMR spectra were recorded on a Bruker UltraShield 500 spectrometer, and all shifts are quoted with respect to TMS. The fine splitting of pyridyl or phenyl ring AA′BB′ patterns is ignored, and the signals are reported as simple doublets, with "*J* values" referring to the two most intense peaks. Elemental analyses were performed by the Microanalytical Laboratory, University of Manchester, and UV−vis spectra were obtained by using a Shimadzu UV-2401 PC spectrophotometer. Cyclic voltammetric measurements were performed by using an EG&G PAR model 283 potentiostat/galvanostat. A single-compartment cell was used with a Ag/AgCl reference electrode (3 M NaCl, saturated AgCl) separated by a salt bridge from a 2 mm disk glassy carbon working electrode and Pt wire auxiliary electrode. Acetonitrile was freshly distilled (from CaH_2), and $[N(C_4H_9\text{-}n)_4]PF_6$, as supplied from Aldrich, was used as the supporting electrolyte. Solutions containing about 10^{-3} M analyte (0.1 M electrolyte) were deaerated by purging with N_2. All $E_{1/2}$ values were calculated from $(E_{pa} + E_{pc})/2$ at a scan rate of 200 mV s^{-1}.

Synthesis of *N*-(2,4-Dinitrophenyl)-4,4′-bipyridinium Tetraphenylborate, [2,4-DNPhQ$^+$]BPh_4. A solution of ([2,4-DNPhQ$^+$]-Cl·0.5EtOH·0.25H_2O (1.00 g, 2.59 mmol) in water (30 mL) was treated with saturated aqueous $NaBPh_4$, and the resulting yellow precipitate was filtered off, washed with water, diethyl ether, and hexane and dried: 1.36 g, 82%; δ_H ($(CD_3)_2CO$) 9.27 (1 H, d, $J_{3,5}$ = 2.6 Hz, 2,4-DNPh-H^3), 9.18 (2 H, d, *J* = 7.0 Hz, C_5H_4N), 8.94−8.92 (3 H, 2,4-DNPh-H^5 and C_5H_4N), 8.71 (2 H, d, *J* = 6.9 Hz, C_5H_4N), 8.27 (1 H, d, $J_{5,6}$ = 8.6 Hz, 2,4-DNPh-H^6), 8.01 (2 H, d, *J* = 6.3 Hz, C_5H_4N), 7.35−7.31 (8 H, BPh_4-H^{3,5}), 6.89 (8 H, t, *J* = 7.4 Hz, BPh_4-H^{2,6}), 6.74 (4 H, t, *J* = 7.7 Hz, BPh_4-H^4). Anal. Calcd. (%) for $C_{40}H_{31}BN_4O_4$: C, 74.8; H, 4.9; N, 8.7. Found: C, 74.5; H, 4.9; N, 8.6.

Synthesis of *N*-*n*-Hexyl-4,4′-bipyridinium Tetraphenylborate, [$C_6H_{13}Q^+$]BPh_4. A solution of 4,4′-bipyridyl (2.00 g, 12.8 mmol) and 1-iodo-*n*-hexane (0.95 mL, 6.44 mmol) in acetone (20 mL) was heated under reflux for 4 h. The resulting red solution was cooled to room temperature, diethyl ether was added, and the orange precipitate was filtered off, washed with diethyl ether and dried. This crude iodide salt was dissolved in water (20 mL) and added slowly to aqueous $NaBPh_4$ (ca. 0.04 M). The resulting pale yellow solid was filtered off, washed with water, then diethyl ether, and dried: 1.41 g, 39%; δ_H ($(CD_3)_2CO$) 8.83 (2 H, d, *J* = 6.3 Hz, C_5H_4N), 8.79 (2 H, d, *J* = 7.0 Hz, C_5H_4N), 8.33 (2 H, d, *J* = 6.6 Hz, C_5H_4N), 7.83 (2 H, d, *J* = 6.3 Hz, C_5H_4N), 7.39−7.35 (8 H, BPh_4-H^{3,5}), 6.91 (8 H, t, *J* = 7.4 Hz, BPh_4-H^{2,6}), 6.76 (4 H, t, *J* = 7.1 Hz, BPh_4-H^4), 4.60 (2 H, t, *J* = 7.6 Hz, CH_2−N$^+$), 2.07−2.01 (2 H, CH_2 (overlaps solvent signal)), 1.44−1.31 (6 H, C_3H_6), 0.88 (3 H, t, *J* = 7.1 Hz, Me). Anal. Calcd (%) for $C_{40}H_{41}BN_2$: C, 85.7; H, 7.4; N, 5.0. Found: C, 85.8; H, 7.6; N, 4.9.

Synthesis of *N*-*n*-Hexyl-4,4′-bipyridinium Triflate, [$C_6H_{13}Q^+$]-CF_3SO_3. To a solution of crude [$C_6H_{13}Q^+$]I (see above; 214 mg, 0.581 mmol) in dichloromethane (10 mL) was added $AgCF_3SO_3$ (149 mg, 0.581 mmol). Because of the low solubility of $AgCF_3SO_3$, the reaction was activated for 1 min by using an ultrasound bath and then stirred for 16 h at room temperature. The mixture was filtered and the AgI precipitate washed with dichloromethane then diethyl ether. The filtrate was reduced to a small volume under vacuum, diethyl ether added, and the resulting white precipitate was filtered off, washed with diethyl ether, and dried: 213 mg, 94%; δ_H ($CDCl_3$) 9.05 (2 H, d, *J* = 6.9 Hz, C_5H_4N), 8.87 (2 H, d, *J* = 6.3 Hz, C_5H_4N), 8.30 (2 H, d, *J* = 7.0 Hz, C_5H_4N), 7.71 (2 H, d, *J* = 6.3 Hz, C_5H_4N), 4.71 (2 H, t, *J* = 7.4 Hz, CH_2−N$^+$), 2.06−1.99 (2 H, CH_2), 1.40−1.25 (6 H, C_3H_6), 0.86 (3 H, t, *J* = 7.1 Hz, Me). Anal. Calcd (%) for $C_{17}H_{21}F_3N_2O_3S$: C, 52.3; H, 5.4; N, 7.2. Found: C, 52.0; H, 5.4; N, 7.0.

Synthesis of *N*-Hexyl-4,4′-bipyridinium Hexafluorophosphate, [$C_6H_{13}Q^+$]PF_6. To a solution of crude [$C_6H_{13}Q^+$]I (see above; 315 mg, 0.855 mmol) in water (10 mL) was added saturated aqueous NH_4PF_6. The resulting white precipitate was filtered off, washed with water and dried: 285 mg, 86%; δ_H ($(CD_3)_2CO$) 9.30 (2 H, d, *J* = 6.7 Hz, C_5H_4N), 8.87 (2 H, d, *J* = 6.0 Hz, C_5H_4N), 8.67 (2 H, d, *J* = 6.6 Hz, C_5H_4N), 7.99 (2 H, d, *J* = 6.3 Hz, C_5H_4N), 4.90 (2 H, t, *J* = 7.6 Hz, CH_2−N$^+$), 2.22−2.16 (2 H, CH_2), 1.51−1.47 (2 H, CH_2), 1.41−1.30 (4 H, C_2H_4), 0.88 (3 H, t, *J* = 7.1 Hz, Me). Anal. Calcd (%) for $C_{16}H_{21}F_6N_2P$: C, 49.8; H, 5.5; N, 7.3. Found: C, 49.5; H, 5.7; N, 7.1.

Synthesis of *N*-*n*-Hexadecyl-4,4′-bipyridinium Iodide, [$C_{16}H_{33}Q^+$]I. A solution of 4,4′-bipyridyl (2.00 g, 12.8 mmol) and 1-iodo-*n*-hexadecane (2.30 g, 6.53 mmol) in acetone (30 mL) was heated under reflux for 6 h. The solvent was reduced to a small volume under vacuum, diethyl ether added, and the resulting yellow precipitate was filtered off, washed with diethyl ether and dried: 1.33 g, 40%; δ_H ($CDCl_3$) 9.42 (2 H, d, *J* = 7.0 Hz, C_5H_4N), 8.90 (2 H, d, *J* = 6.0 Hz, C_5H_4N), 8.35 (2 H, d, *J* = 6.9 Hz, C_5H_4N), 7.70 (2 H, d, *J* = 6.4 Hz,

dx.doi.org/10.1021/ic202145b | Inorg. Chem. 2011, 50, 12886−12899

C_5H_4N), 4.98 (2 H, t, J = 7.6 Hz, CH_2-N^+), 2.12−2.06 (2 H, CH_2), 1.45−1.22 (26 H, $C_{13}H_{26}$), 0.88 (3 H, t, J = 7.0 Hz, Me). Anal. Calcd (%) for $C_{26}H_{41}IN_2$: C, 61.4; H, 8.1; N, 5.5. Found: C, 61.1; H, 8.3; N, 5.4.

Synthesis of *N*-*n*-Hexadecyl-4,4′-bipyridinium Hexafluorophosphate, [$C_{16}H_{33}Q^+$]PF_6. A solution of [$C_{16}H_{33}Q^+$]I (500 mg, 0.983 mmol) in methanol (20 mL) was added slowly to saturated aqueous NH_4PF_6. The resulting white solid was filtered off, washed with water and dried: 492 mg, 95%; δ_H ($(CD_3)_2CO$) 9.32 (2 H, d, J = 6.5 Hz, C_5H_4N), 8.89 (2 H, d, J = 6.0 Hz, C_5H_4N), 8.69 (2 H, d, J = 7.0 Hz, C_5H_4N), 8.01 (2 H, d, J = 6.0 Hz, C_5H_4N), 4.91 (2 H, t, J = 7.5 Hz, CH_2-N^+), 2.23−2.16 (2 H, CH_2), 1.51−1.43 (2 H, CH_2), 1.42−1.36 (2 H, CH_2), 1.35−1.22 (22 H, $C_{11}H_{22}$), 0.87 (3 H, t, J = 6.8 Hz, Me). Anal. Calcd (%) for $C_{26}H_{41}F_6N_2P{\cdot}0.5H_2O$: C, 58.3; H, 7.9; N, 5.2. Found: C, 58.6; H, 7.9; N, 5.1.

Synthesis of *N*-*n*-Hexadecyl-4,4′-bipyridinium Triflate, [$C_{16}H_{33}Q^+$]CF_3SO_3. This compound was prepared in a manner similar to [$C_6H_{13}Q^+$]CF_3SO_3 by using [$C_{16}H_{33}Q^+$]I (500 mg, 0.983 mmol) and $AgCF_3SO_3$ (252 mg, 0.981 mmol) to afford a white solid: 496 mg, 95%; δ_H ($CDCl_3$) 9.01 (2 H, d, J = 7.0 Hz, C_5H_4N), 8.88 (2 H, d, J = 6.4 Hz, C_5H_4N), 8.27 (2 H, d, J = 7.0 Hz, C_5H_4N), 7.67 (2 H, d, J = 6.0 Hz, C_5H_4N), 4.70 (2 H, t, J = 7.6 Hz, CH_2-N^+), 2.05−1.99 (2 H, CH_2), 1.38−1.22 (26 H, $C_{13}H_{26}$), 0.88 (3 H, t, J = 6.9 Hz, Me). Anal. Calcd (%) for $C_{27}H_{41}F_3N_2O_3S$: C, 61.1; H, 7.8; N, 5.3. Found: C, 60.8; H, 8.1; N, 5.2.

Synthesis of *N*-(4-*n*-Hexylphenyl)-4,4′-bipyridinium Hexafluorophosphate, [4-$C_6H_{13}PhQ^+$]PF_6. A solution of [2,4-$DNPhQ^+$]Cl·0.5EtOH·0.25H_2O (372 mg, 0.963 mmol) and 4-(*n*-hexyl)-aniline (1.00 mL, 5.18 mmol) in ethanol (30 mL) was heated under reflux for 3 h. The solvent was evaporated to a small volume, acetone was added, and the mixture stored at 4 °C for 16 h. The pale brown precipitate was filtered off, washed with acetone, and dried. The solid was dissolved in water, and brown material was removed by filtration, leaving a yellow filtrate to which was added slowly saturated aqueous NH_4PF_6. The resulting cream-colored precipitate was filtered off, washed with water, and dried: 270 mg, 61%; δ_H ($(CD_3)_2CO$) 9.49 (2 H, d, J = 6.6 Hz, C_5H_4N), 8.91 (2 H, d, J = 6.0 Hz, C_5H_4N), 8.82 (2 H, d, J = 7.0 Hz, C_5H_4N), 8.07 (2 H, d, J = 6.0 Hz, C_5H_4N), 7.92 (2 H, d, J = 8.6 Hz, C_6H_4), 7.65 (2 H, d, J = 8.2 Hz, C_6H_4), 2.82 (2 H, t, J = 7.5 Hz, CH_2−Ph), 1.75−1.69 (2 H, CH_2), 1.42−1.31 (6 H, C_3H_6), 0.89 (3 H, t, J = 7.1 Hz, Me). Anal. Calcd (%) for $C_{22}H_{25}F_6N_2P$: C, 57.1; H, 5.5; N, 6.1. Found: C, 56.9; H, 5.3; N, 5.7.

Synthesis of *N*-(4-*n*-Hexadecylphenyl)-4,4′-bipyridinium Hexafluorophosphate, [4-$C_{16}H_{33}PhQ^+$]PF_6. A solution of [2,4-$DNPhQ^+$]Cl·0.5EtOH·0.25H_2O (550 mg, 1.42 mmol) and 4-(*n*-hexadecyl)aniline (730 mg, 2.45 mmol) in ethanol (22 mL) was heated under reflux for 24 h. After cooling to room temperature, the precipitate was filtered off, washed thoroughly with diethyl ether, and dried. The cream-colored solid was dissolved in methanol and added slowly to saturated aqueous NH_4PF_6. The resulting solid precipitate was filtered off, washed with water, and dried: 850 mg, 99%; δ_H ($(CD_3)_2CO$) 9.51 (2 H, d, J = 6.5 Hz, C_5H_4N), 8.92 (2 H, d, J = 5.5 Hz, C_5H_4N), 8.84 (2 H, d, J = 6.5 Hz, C_5H_4N), 8.08 (2 H, d, J = 5.5 Hz, C_5H_4N), 7.92 (2 H, d, J = 8.5 Hz, C_6H_4), 7.66 (2 H, d, J = 8.0 Hz, C_6H_4), 2.82 (2 H, t, J = 7.5 Hz, CH_2−Ph), 1.73−1.70 (2 H, CH_2), 1.48−1.24 (26 H, $C_{13}H_{26}$), 0.87 (3 H, t, J = 6.5 Hz, Me). Anal. Calcd (%) for $C_{32}H_{45}F_6N_2P$: C, 63.8; H, 7.5; N, 4.7. Found: C, 63.3; H, 7.5; N, 4.4.

Synthesis of *N*-(4-*n*-Hexadecyloxycarbonylphenyl)-4,4′-bipyridinium Hexafluorophosphate, [4-$C_{16}H_{33}O_2CPhQ^+$]PF_6. A mixture of [2,4-$DNPhQ^+$]BPh_4 (642 mg, 1.00 mmol) and 4-(*n*-hexadecyloxycarbonyl)aniline (542 mg, 1.50 mmol) was dissolved in ethanol (20 mL). Triethylamine (0.17 mL, 1.22 mmol) was added, and the resulting dark solution heated under reflux for 24 h. The solvent was evaporated to dryness, and the crude solid dissolved in acetone. The cloudy solution was filtered, and the yellow solid collected was identified as 4,4′-bis(*n*-hexadecyloxycarbonyl)azobenzene: 25 mg, 4%; δ_H ($CDCl_3$) 8.22 (4 H, d, J = 8.2 Hz, C_6H_4), 8.00 (4 H, d, J = 8.2 Hz, C_6H_4), 4.37 (4 H, t, J = 6.5 Hz, $2CH_2O$), 1.83−1.77 (4 H, $2CH_2$), 1.50−1.44 (4 H, $2CH_2$), 1.42−1.23 (52 H, $2C_{13}H_{26}$), 0.88 (6 H, t, J = 6.8 Hz, 2Me). Anal. Calcd (%) for $C_{46}H_{74}N_2O_4{\cdot}2H_2O$: C, 73.2; H, 10.4; N, 3.7. Found: C, 73.5; H, 9.8; N, 3.7. To the filtrate was added solid [$N(C_4H_9\text{-}n)_4$]Cl to precipitate the desired cation as its chloride salt which was then dissolved in methanol and poured into saturated aqueous NH_4PF_6. The cream-colored product was filtered off, washed thoroughly with water, and dried: 305 mg, 47%; δ_H ($(CD_3)_2CO$) 9.60 (2 H, d, J = 6.6 Hz, C_5H_4N), 8.92 (2 H, d, J = 5.8 Hz, C_5H_4N), 8.90 (2 H, d, J = 6.6 Hz, C_5H_4N), 8.39 (2 H, d, J = 8.5 Hz, C_6H_4), 8.19 (2 H, d, J = 8.5 Hz, C_6H_4), 8.09 (2 H, d, J = 5.8 Hz, C_5H_4N), 4.41 (2 H, t, J = 6.6 Hz, CH_2O), 1.86−1.79 (2 H, CH_2), 1.53−1.46 (2 H, CH_2), 1.44−1.23 (26 H, $C_{13}H_{26}$), 0.87 (3 H, t, J = 6.5 Hz, Me). Anal. Calcd (%) for $C_{33}H_{45}F_6N_2O_2P{\cdot}0.5H_2O$: C, 60.5; H, 7.1; N, 4.3. Found: C, 60.5; H, 7.4; N, 4.2.

Synthesis of *N*-(4-(*n*-Hexadecyl(methyl)sulfamoyl)-phenyl)-4,4′-bipyridinium Hexafluorophosphate, [4-$C_{16}H_{33}NMeSO_2PhQ^+$]PF_6. This compound was prepared and purified in a manner similar to [4-$C_{16}H_{33}O_2CPhQ^+$]PF_6 by using 4-amino-*N*-*n*-hexadecyl-*N*-methylbenzenesulfonamide (615 mg, 1.50 mmol) instead of 4-*n*-hexadecyloxycarbonylaniline to afford a cream-colored solid: 140 mg, yield 20%; δ_H ($(CD_3)_2CO$) 9.63 (2 H, d, J = 6.5 Hz, C_5H_4N), 8.93 (4 H, d, J = 6.0 Hz, $2C_5H_4N$), 8.31 (2 H, d, J = 8.5 Hz, C_6H_4), 8.23 (2 H, d, J = 8.5 Hz, C_6H_4), 8.10 (2 H, d, J = 5.5 Hz, C_5H_4N), 3.13 (2 H, t, J = 7.0 Hz, CH_2N), 2.81 (3 H, s, Me−N), 1.64−1.56 (2 H, CH_2), 1.39−1.22 (26 H, $C_{13}H_{26}$), 0.87 (3 H, t, J = 7.0 Hz, Me). Anal. Calcd (%) for $C_{33}H_{48}F_6N_3O_2PS$: C, 57.0; H, 7.0; N, 6.0. Found: C, 57.0; H, 7.0; N, 6.0.

Synthesis of *N*-(2-(*n*-Perfluorooctyl)ethyl)-4,4′-bipyridinium Hexafluorophosphate, [$C_8F_{17}C_2H_4Q^+$]PF_6. A solution of 4,4′-bipyridyl (410 mg, 2.63 mmol) and 1-iodo-2-(perfluoro-*n*-octyl)ethane (1.00 g, 1.74 mmol) in DMF (30 mL) was heated under reflux for 24 h. The resulting orange solution was poured into saturated aqueous NH_4PF_6 and the resulting white precipitate was filtered off, washed with water then diethyl ether and dried: 410 mg, 31%; δ_H ($(CD_3)_2CO$) 9.52 (2 H, d, J = 6.0 Hz, C_5H_4N), 8.89 (2 H, d, J = 5.0 Hz, C_5H_4N), 8.78 (2 H, d, J = 6.5 Hz, C_5H_4N), 8.01 (2 H, d, J = 5.0 Hz, C_5H_4N), 5.40 (2 H, t, J = 7.3 Hz, CH_2-N^+), 3.51−3.36 (2 H, m, CH_2-CF_2). Anal. Calcd (%) for $C_{20}H_{12}F_{23}N_2P$: C, 32.1; H, 1.6; N, 3.7. Found: C, 31.8; H, 1.1; N, 3.8.

Synthesis of *N*-(4-(*n*-Heptadecafluorooctyl)phenyl)-4,4′-bipyridinium Hexafluorophosphate, [4-$C_8F_{17}PhQ^+$]PF_6. This compound was prepared and purified in a manner similar to [4-$C_{16}H_{33}O_2CPhQ^+$]PF_6 by using 4-(*n*-heptadecafluorooctyl)aniline (760 mg, 1.49 mmol) instead of 4-(*n*-hexadecyloxycarbonyl)aniline to afford a pale brown solid: 280 mg, 35%; δ_H ($(CD_3)_2CO$) 9.66 (2 H, d, J = 6.5 Hz, C_5H_4N), 8.93 (4 H, d, J = 6.0 Hz, $2C_5H_4N$), 8.37 (2 H, d, J = 8.5 Hz, C_6H_4), 8.21 (2 H, d, J = 8.5 Hz, C_6H_4), 8.11 (2 H, d, J = 6.0 Hz, C_5H_4N). Anal. Calcd (%) for $C_{24}H_{12}F_{23}N_2P{\cdot}0.5H_2O$: C, 35.8; H, 1.6; N, 3.5. Found: C, 35.5; H, 1.1; N, 3.4.

Synthesis of 4-(Perfluoro-*n*-octylthio)aniline. A suspension of 4-aminothiophenol (500 mg, 3.99 mmol) and K_2CO_3 (1.1 g, 7.96 mmol) in dimethylformamide (DMF, 20 mL) was stirred at room temperature for 10 min. 1-Iodoperfluoro-*n*-octane (1.1 mL, 4.16 mmol) was added and the mixture stirred at room temperature for 24 h, after which time it was a green-brown color with suspended solid material. Ethyl acetate was added, the mixture was extracted with water followed by brine, and the organic phase was dried over $MgSO_4$. Purification was effected by column chromatography on silica gel, eluting first with dichloromethane and then with 20% ethyl acetate/dichloromethane. The first major fraction eluted was evaporated to give a white solid: 810 mg; 37%; δ_H ($CDCl_3$) 7.41 (2 H, d, J = 8.5 Hz, C_6H_4), 6.66 (2 H, d, J = 8.5 Hz, C_6H_4), 3.95 (2 H, br s, NH_2). Anal. Calcd (%) for $C_{14}H_6F_{17}NS$: C, 31.0; H, 1.1; N, 2.6. Found: C, 30.8; H, 0.7; N, 2.6.

Synthesis of *N*-(4-(*n*-Heptadecafluorooctylsulfanyl)phenyl)-4,4′-bipyridinium Hexafluorophosphate, [4-$C_8F_{17}SPhQ^+$]PF_6. This compound was prepared and purified in a manner similar to [4-$C_{16}H_{33}O_2CPhQ^+$]PF_6 by using 4-(perfluoro-*n*-octylthio)aniline (815 mg, 1.50 mmol) instead of 4-(*n*-hexadecyloxycarbonyl)aniline to afford a cream-colored solid: 165 mg, 20%; δ_H ($(CD_3)_2CO$) 9.65 (2 H, d, J = 7.0 Hz, C_5H_4N), 8.93−8.91 (4 H, $2C_5H_4N$), 8.25 (2 H, d, J = 8.5 Hz, C_6H_4), 8.22 (2 H, d, J = 9.0 Hz, C_6H_4), 8.11 (2 H, d, J = 6.0 Hz,

C_5H_4N). Anal. Calcd (%) for $C_{24}H_{12}F_{23}N_2PS{\cdot}0.5H_2O$: C, 34.4; H, 1.6; N, 3.4. Found: C, 34.3; H, 1.1; N, 3.2.

Synthesis of $[Ru^{II}(NH_3)_5(C_6H_{13}Q^+)][PF_6]_3$ (2). A solution of $[Ru^{II}(NH_3)_5(H_2O)][PF_6]_2$ (100 mg, 0.202 mmol) and $[C_6H_{13}Q^+]PF_6$ (75 mg, 0.194 mmol) in acetone (5 mL) was stirred at room temperature in the dark for 4 h. Diethyl ether was added to the resulting deep blue solution to give a dark red-purple precipitate which was filtered off and washed with diethyl ether. Purification was effected by reprecipitations from acetone/saturated aqueous NH_4PF_6 and then from acetone/diethyl ether to afford a dark purple solid: 88 mg, 53%; δ_H ($(CD_3)_2CO$) 9.15 (4 H, d, J = 6.7 Hz, C_5H_4N), 8.70 (2 H, d, J = 6.7 Hz, C_5H_4N), 7.87 (2 H, d, J = 6.6 Hz, C_5H_4N), 4.79 (2 H, t, J = 7.6 Hz, $CH_2{-}N^+$), 3.52 (3 H, s, NH_3), 2.67 (12 H, s, $4NH_3$), 2.19–2.13 (2 H, CH_2), 1.50–1.37 (2 H, CH_2), 1.40–1.29 (4 H, C_2H_4), 0.88 (3 H, t, J = 7.0 Hz, Me). Anal. Calcd (%) for $C_{16}H_{36}F_{18}N_7P_3Ru$: C, 22.3; H, 4.2; N, 11.4. Found: C, 22.7; H, 3.9; N, 11.0.

Synthesis of $[Ru^{II}(NH_3)_5(4\text{-}C_6H_{13}PhQ^+)][PF_6]_3$ (3). This compound was prepared and purified in a manner similar to **2** by using $[4\text{-}C_6H_{13}PhQ^+]PF_6$ (94 mg, 0.203 mmol) instead of $[C_6H_{13}Q^+]PF_6$ to afford a dark purple solid: 83 mg, 44%; δ_H ($(CD_3)_2CO$) 9.33 (2 H, d, J = 7.0 Hz, C_5H_4N), 9.21 (2 H, d, J = 6.6 Hz, C_5H_4N), 8.85 (2 H, d, J = 7.0 Hz, C_5H_4N), 7.97 (2 H, d, J = 6.9 Hz, C_5H_4N), 7.88 (2 H, d, J = 8.5 Hz, C_6H_4), 7.63 (2 H, d, J = 8.5 Hz, C_6H_4), 3.61 (3 H, s, NH_3), 2.80 (2 H, t, J = 7.7 Hz, $CH_2{-}Ph$), 2.71 (12 H, s, $4NH_3$), 1.74–1.68 (2 H, CH_2), 1.43–1.30 (6 H, C_3H_6), 0.90 (3 H, t, J = 7.0 Hz, Me). Anal. Calcd (%) for $C_{22}H_{40}F_{18}N_7P_3Ru$: C, 28.2; H, 4.3; N, 10.5. Found: C, 28.3; H, 4.3; N, 10.4.

General Procedure for Synthesis of Complex Salts $[Ru^{II}(NH_3)_5(L^A)][PF_6]_3$ with Long Hydrocarbon or Fluorocarbon Chain Substituents. A solution of $[Ru^{II}(NH_3)_5(H_2O)][PF_6]_2$ (100 mg, 0.202 mmol) and the appropriate L^A proligand PF_6^- salt (0.120 mmol) in acetone (10 mL) was stirred at room temperature in the dark for 12 h. The resulting dark blue solution was added to saturated aqueous NH_4PF_6 and the dark purple solid precipitate was filtered off, washed thoroughly with water and dried.

Data for $[Ru^{II}(NH_3)_5(C_{16}H_{33}Q^+)][PF_6]_3$ (4). Yield: 100 mg, 83%; δ_H ($(CD_3)_2CO$) 9.14–9.22 (4 H, C_5H_4N), 8.73 (2 H, d, J = 6.5 Hz, C_5H_4N), 7.88 (2 H, d, J = 6.5 Hz, C_5H_4N), 4.79 (2 H, t, J = 7.5 Hz, $CH_2{-}N^+$), 3.59 (3 H, s, NH_3), 2.71 (12 H, s, $4NH_3$), 2.12–2.07 (2 H, CH_2), 1.25–1.08 (26 H, $C_{13}H_{26}$), 0.87 (3 H, t, J = 7.0 Hz, Me). Anal. Calcd (%) for $C_{26}H_{56}F_{18}N_7P_3Ru$: C, 31.1; H, 5.6; N, 9.8. Found: C, 31.3; H, 5.7; N, 9.5.

Data for $[Ru^{II}(NH_3)_5(4\text{-}C_{16}H_{33}PhQ^+)][PF_6]_3$ (5). Yield: 124 mg, 96%; δ_H ($(CD_3)_2CO$) 9.35 (2 H, d, J = 6.5 Hz, C_5H_4N), 9.22 (2 H, d, J = 7.0 Hz, C_5H_4N), 8.86 (2 H, d, J = 7.0 Hz, C_5H_4N), 7.97 (2 H, d, J = 6.5 Hz, C_5H_4N), 7.88 (2 H, d, J = 8.5 Hz, C_6H_4), 7.63 (2 H, d, J = 8.0 Hz, C_6H_4), 3.63 (3 H, s, NH_3), 2.79 (2 H, t, J = 7.7 Hz, $CH_2{-}Ph$), 2.73 (12 H, s, $4NH_3$), 1.74–1.67 (2 H, CH_2), 1.43–1.22 (26 H, $C_{13}H_{26}$), 0.88 (3 H, t, J = 7.0 Hz, Me). Anal. Calcd (%) for $C_{32}H_{60}F_{18}N_7P_3Ru{\cdot}C_3H_6O$: C, 37.0; H, 5.9; N, 8.6. Found: C, 36.6; H, 6.0; N, 8.7. The residual acetone included in the isolated product is also evidenced by an extra singlet at 2.09 ppm (integrating to 6 H) in the ^{1}H NMR spectrum. A small portion of the product was converted into its chloride salt $[Ru^{II}(NH_3)_5(C_{16}H_{33}PhQ^+)]Cl_3$ (**5-Cl**) by the addition of solid $[N(C_4H_9\text{-}n)_4]Cl$ to an acetone solution; the resulting dark purple solid was highly hygroscopic and therefore was not analyzed, but used directly for crystallization experiments (see below).

Data for $[Ru^{II}(NH_3)_5(4\text{-}C_{16}H_{33}O_2CPhQ^+)][PF_6]_3$ (6). Yield: 128 mg, 95%; δ_H ($(CD_3)_2CO$) 9.42 (2 H, d, J = 6.5 Hz, C_5H_4N), 9.23 (2 H, d, J = 6.5 Hz, C_5H_4N), 8.91 (2 H, d, J = 6.5 Hz, C_5H_4N), 8.37 (2 H, d, J = 8.5 Hz, C_6H_4), 8.14 (2 H, d, J = 8.5 Hz, C_6H_4), 7.98 (2 H, d, J = 7.0 Hz, C_5H_4N), 4.40 (2 H, t, J = 6.8 Hz, CH_2O), 3.67 (3 H, s, NH_3), 2.73 (12 H, s, $4NH_3$), 1.85–1.78 (2 H, CH_2), 1.53–1.45 (2 H, CH_2), 1.43–1.22 (24 H, $C_{12}H_{24}$), 0.87 (3 H, t, J = 6.8 Hz, Me). Anal. Calcd (%) for $C_{33}H_{60}F_{18}N_7O_2P_3Ru$: C, 35.3; H, 5.4; N, 8.7. Found: C, 35.4; H, 5.4; N, 8.5.

Data for $[Ru^{II}(NH_3)_5(4\text{-}C_{16}H_{33}NMeSO_2PhQ^+)][PF_6]_3$ (7). Yield: 126 mg, 87%; δ_H ($(CD_3)_2CO$) 9.42 (2 H, d, J = 6.5 Hz, C_5H_4N), 9.23 (2 H, d, J = 7.0 Hz, C_5H_4N), 8.92 (2 H, d, J = 7.0 Hz, C_5H_4N), 8.25 (2 H, d, J = 8.5 Hz, C_6H_4), 8.19 (2 H, d, J = 8.5 Hz, C_6H_4), 7.98 (2 H, d, J = 6.5 Hz, C_5H_4N), 3.69 (3 H, s, NH_3), 3.11 (2 H, t, J = 7.3 Hz, CH_2N), 2.82 (3 H, s, Me–N), 2.74 (12 H, s, $4NH_3$), 1.64–1.56 (2 H, CH_2), 1.38–1.24 (26 H, $C_{13}H_{26}$), 0.87 (3 H, t, J = 6.8 Hz, Me). Anal. Calcd (%) for $C_{33}H_{63}F_{18}N_8O_2P_3RuS{\cdot}0.5C_3H_6O$: C, 34.5; H, 5.5; N, 9.3. Found: C, 34.7; H, 5.9; N, 9.2. The residual acetone included in the isolated product is also evidenced by an extra singlet at 2.09 ppm (integrating to 3 H) in the ^{1}H NMR spectrum.

Data for $[Ru^{II}(NH_3)_5(C_8F_{17}C_2H_4Q^+)][PF_6]_3$ (8). Yield: 113 mg, 77%; δ_H ($(CD_3)_2CO$) 9.33 (2 H, d, J = 7.0 Hz, C_5H_4N), 9.18 (2 H, d, J = 7.0 Hz, C_5H_4N), 8.79 (2 H, d, J = 7.0 Hz, C_5H_4N), 7.90 (2 H, d, J = 7.0 Hz, C_5H_4N), 5.26 (2 H, t, J = 7.3 Hz, $CH_2{-}N^+$), 3.59 (3 H, s, NH_3), 3.32–3.45 (2 H, $CH_2{-}CF_2$), 2.70 (12 H, s, $4NH_3$). Anal. Calcd (%) for $C_{20}H_{27}F_{35}N_7P_3Ru$: C, 19.6; H, 2.2; N, 8.0. Found: C, 20.1; H, 1.8; N, 7.7.

Data for $[Ru^{II}(NH_3)_5(4\text{-}C_8F_{17}PhQ^+)][PF_6]_3$ (9). Yield: 140 mg, 92%; δ_H ($(CD_3)_2CO$) 9.47 (2 H, d, J = 7.0 Hz, C_5H_4N), 9.24 (2 H, d, J = 6.5 Hz, C_5H_4N), 8.93 (2 H, d, J = 7.0 Hz, C_5H_4N), 8.31 (2 H, d, J = 8.5 Hz, C_6H_4), 8.17 (2 H, d, J = 8.5 Hz, C_6H_4), 7.99 (2 H, d, J = 6.5 Hz, C_5H_4N), 3.68 (3 H, s, NH_3), 2.74 (12 H, s, $4NH_3$). Anal. Calcd (%) for $C_{24}H_{27}F_{35}N_7P_3Ru$: C, 22.7; H, 2.1; N, 7.7. Found: C, 23.0; H, 1.8; N, 7.4.

Data for $[Ru^{II}(NH_3)_5(4\text{-}C_8F_{17}SPhQ^+)][PF_6]_3$ (10). Yield: 153 mg, 96%; δ_H ($(CD_3)_2CO$) 9.45 (2 H, d, J = 7.0 Hz, C_5H_4N), 9.23 (2 H, d, J = 6.5 Hz, C_5H_4N), 8.92 (2 H, d, J = 6.5 Hz, C_5H_4N), 8.19 (4 H, s, C_6H_4), 7.99 (2 H, d, J = 6.0 Hz, C_5H_4N), 3.68 (3 H, s, NH_3), 2.74 (12 H, s, $4NH_3$). Anal. Calcd (%) for $C_{24}H_{27}F_{35}N_7P_3RuS{\cdot}0.5C_3H_6O$: C, 23.0; H, 2.3; N, 7.4. Found: C, 23.3; H, 1.8; N, 6.9. The residual acetone included in the isolated product is also evidenced by an extra singlet at 2.09 ppm (integrating to 3 H) in the ^{1}H NMR spectrum.

X-ray Structural Determination. Suitable pale yellow prismatic crystals of $[C_6H_{13}Q^+]BPh_4$ and colorless plate-like crystals of $[C_6H_{13}Q^+]CF_3SO_3$ were grown by diffusion of toluene into dichloromethane solutions at room temperature. Suitable dark blue needle-like crystals of **5-Cl**·3.25H_2O were grown by diffusion of acetone into an aqueous solution at room temperature. The data for $[C_6H_{13}Q^+]BPh_4$ and $[C_6H_{13}Q^+]CF_3SO_3$ were collected on a Bruker APEX CCD X-ray diffractometer by using graphite-monochromated, Mo$K\alpha$ radiation (wavelength = 0.71073 Å). Because the crystals of **5-Cl**·3.25H_2O diffracted extremely weakly, the data in this case were collected by using a Bruker APEX II CCD diffractometer (wavelength = 0.6945 Å) in Station 9.8 at the Synchrotron Radiation Source, Daresbury Laboratory, Warrington, Cheshire, U.K. Even so, the data were very weak at higher resolution and were therefore cut at θ = 21.63°. Data processing was carried out by using the Bruker SAINT[19] software package and a semiempirical absorption correction was applied by using SADABS.[19] The structures were solved by direct methods and refined by full-matrix least-squares on all F_0^2 data by using SHELXS-97[20] and SHELXL-97.[21] All non-H atoms were refined anisotropically, with H atoms bonded to C or N included in calculated positions by using the riding method; those bonded to the water O atoms could not be located. All other calculations were carried out by using the SHELXTL package.[22] For $[C_6H_{13}Q^+]BPh_4$, there was disorder of C13–C14 with occupancies constrained to sum to 1.0; the occupancy of the highest fraction refined to a value of 0.902(4). There are two independent cations in the unit cell of $[C_6H_{13}Q^+]CF_3SO_3$. The structure of **5-Cl**·3.25H_2O comprises two complex cations in the asymmetric unit together with six Cl^- ions and eight water molecules, one of the latter at 0.5 occupancy. Crystallographic data and refinement details are presented in Table 1.

Langmuir–Blodgett (LB) Film Deposition. A solution of the complex salt in chloroform (5×10^{-4} M) was spread onto an ultrapure water subphase (resistance larger than 18 MΩ) obtained from a Milli-Q Millipore apparatus. Films of **4** and **5** on simple glass slides and precoated ITO slides were obtained by vertical dipping in a KSV5000 model computer-controlled trough. The substrates were made hydrophilic by being first washed with methanol then boiled in a mixture of aqueous H_2O_2/30% aqueous NH_3 for 20 min and finally rinsed thoroughly with ultrapure water. Film transfer was investigated by the vertical LB dipping method with hydrophilic glass slides at a

dx.doi.org/10.1021/ic202145b | Inorg. Chem. 2011, 50, 12886–12899

Table 1. Crystallographic Data and Refinement Details for Salts $[C_6H_{13}Q^+]BPh_4$, $[C_{16}H_{33}Q^+]CF_3SO_3$, and 5-Cl·3.25$H_2O$

	$[C_6H_{13}Q^+]BPh_4$	$[C_6H_{13}Q^+]CF_3SO_3$	5-Cl·3.25H_2O
empirical formula	$C_{40}H_{41}BN_2$	$C_{17}H_{21}F_3N_2O_3S$	$C_{128}H_{270}Cl_{12}N_{28}O_{15}Ru_4$
fw	560.56	390.42	3271.40
cryst system	monoclinic	monoclinic	triclinic
space group	$P2_1/n$	$P2_1/c$	$P\bar{1}$
a/Å	11.5743(6)	11.6150(2)	9.550(3)
b/Å	17.6392(10)	14.6310(2)	13.767(5)
c/Å	16.0109(9)	22.5870(6)	31.619(10)
α/deg			89.948(4)
β/deg	100.9900(10)	91.2550(7)	84.223(4)
γ/deg			89.510(3)
U/Å^3	3208.9(3)	3837.49(13)	4136(2)
Z	4	8	1
T/K	100(2)	150(2)	100(2)
μ/mm^{-1}	0.066	0.215	0.613
reflns collected	18306	12667	25332
independent reflns (R_{int})	6574 (0.0375)	6757 (0.0578)	11493 (0.0805)
GOF on F^2	1.037	1.009	1.023
final $R1$, $wR2$ [$I > 2\sigma(I)$]	0.0365, 0.0937	0.0835, 0.2236	0.0814, 0.1861
(all data)	0.0497, 0.0972	0.1309, 0.2842	0.1374, 0.2111

constant compression of 20 mN m^{-1}. The efficiency of the transfer process (transfer ratio) is measured by comparing the decrease in the film area on the water/air interface with the area of glass substrate passing through this interface. For **5**, the transfer ratios measured for successive upstrokes and downstrokes are close to unity (±10%), indicating that the transfer process is well-behaved and that the arrangement in the multilayer film is centrosymmetric (Y-type).

SHG and Redox-Switching Measurements. The experimental setup consisted of a modified version of that used previously for hyper-Rayleigh scattering (HRS) studies with electroactive species in solution.[5g,23] All SHG measurements were performed by using a Q-switched Nd^{3+}:YAG laser (model Quanta Ray, Spectra Physics) with 10 ns pulses, repetition rate of 10 Hz and an average output power of 100 mW. The sample was irradiated at a 45° angle of incidence, the input polarization was chosen to be p-polarized, and all the second harmonic light at 532 nm was detected in transmission. For the electrochemical redox-switching experiment, a three bilayer film (where one bilayer contains a layer of **5** and a layer of inactive arachidic acid) was deposited on an ITO-coated glass substrate, serving as a working electrode. This film was placed in a commercially available cuvette (hellma). The sample was oriented at 45° with respect to the incoming laser beam. An Ag wire was used as the reference electrode and a Pt wire as the counter electrode. An electrolyte solution of 0.1 M of $NaBF_4$ in water was used. In this modified electrochemical cell, a potential of 1 V was applied for about 2 min to effect oxidation of the film, while a potential of 0 V was applied to reduce the film to its original state. In all cases, the SHG data were recorded only once the signal had stabilized.

RESULTS AND DISCUSSION

Synthesis. A series of new 4,4′-bipyridinium proligands and their Ru^{II} complexes have been prepared (Figure 1). The creation of LB films requires amphiphilic molecules that generally feature long chain alkyl substituents attached to a polar headgroup, and solubility in an organic solvent (most often $CHCl_3$) combined with complete insolubility in water is essential to allow the formation of a suitable monolayer at an air−water interface. Previous investigations have established that Ru^{II} ammine complexes of the ligands *N*-methyl-4,4′-bipyridinium (MeQ^+) and *N*-phenyl-4,4′-bipyridinium (PhQ^+) show very large β responses,[2i,4,7a,c,17] and the hydrophilic nature of the metal center renders $[Ru^{II}(NH_3)_5(L^A)]^{3+}$ (L^A = a pyridyl pyridinium ligand; MeQ^+ **11** or PhQ^+ **12**)[17] attractive as foundations for the construction of chromophores suitable for LB deposition. In initial studies, we prepared the new *n*-hexyl-substituted proligands $C_6H_{13}Q^+$ and 4-$C_6H_{13}PhQ^+$ and their corresponding $\{Ru^{II}(NH_3)_5\}^{2+}$ complex salts **2** and **3**. However, the latter compounds show only low solubility in $CHCl_3$ and are partially soluble in water; anion metathesis using various species including $CF_3SO_3^-$ and BPh_4^- failed to achieve the desired solubility properties. We therefore turned our attention to the synthesis of related chromophoric salts containing longer *n*-dodecyl chains, as employed by Di Bella and colleagues in **1**.[11] However, the materials prepared still did not display the desired solubility properties, so we settled upon *n*-hexadecyl-substituted systems such as **4** and **5** that show good $CHCl_3$ solubility and appear completely insoluble in water. Experiments with salts containing other anions showed PF_6^- to be the most appropriate and convenient choice among the readily available species. To broaden the scope of this study, several related species containing perfluorooctyl chains have also been studied.

The *N*-alkyl proligands $C_6H_{13}Q^+$, $C_{16}H_{33}Q^+$ and $C_8F_{17}C_2H_4Q^+$ were prepared simply by reacting 4,4′-bpy with the corresponding 1-iodoalkane, and were isolated as their PF_6^- salts for complexation purposes. The *N*-aryl proligands 4-$C_6H_{13}PhQ^+$, 4-$C_{16}H_{33}PhQ^+$, 4-$C_{16}H_{33}O_2CPhQ^+$, 4-$C_{16}H_{33}NMeSO_2PhQ^+$, 4-$C_8F_{17}PhQ^+$, and 4-$C_8F_{17}SPhQ^+$ were synthesized in a fashion similar to PhQ^+, by using Zincke reactions between the *N*-(2,4-dinitrophenyl)-4,4′-bipyridinium (2,4-$DNPhQ^+$) cation and the appropriate aniline derivative. For 4-$C_6H_{13}PhQ^+$ and 4-$C_{16}H_{33}PhQ^+$, the procedure used was analogous to that which we have employed previously to prepare PhQ^+,[17] with $[2,4\text{-}DNPhQ^+]Cl$ as the precursor. However, using only about 1.7 equivalents of the aniline derivative (as opposed to ca. 5.4 equivalents in the case of $[4\text{-}C_6H_{13}PhQ^+]PF_6$) and an extended reaction time of 24 h afforded $[4\text{-}C_{16}H_{33}PhQ^+]PF_6$ in a substantially increased yield that is essentially quantitative. The presence of electron withdrawing 4-substituents on the anilines used in the other syntheses complicated matters because of a combination of decreased nucleophilicity and the poor solubility of the *n*-hexadecyl derivatives in ethanol. The desired proligands were obtained in reasonable yields (ca. 20−50%) by using the new

dx.doi.org/10.1021/ic202145b | Inorg. Chem. 2011, 50, 12886−12899

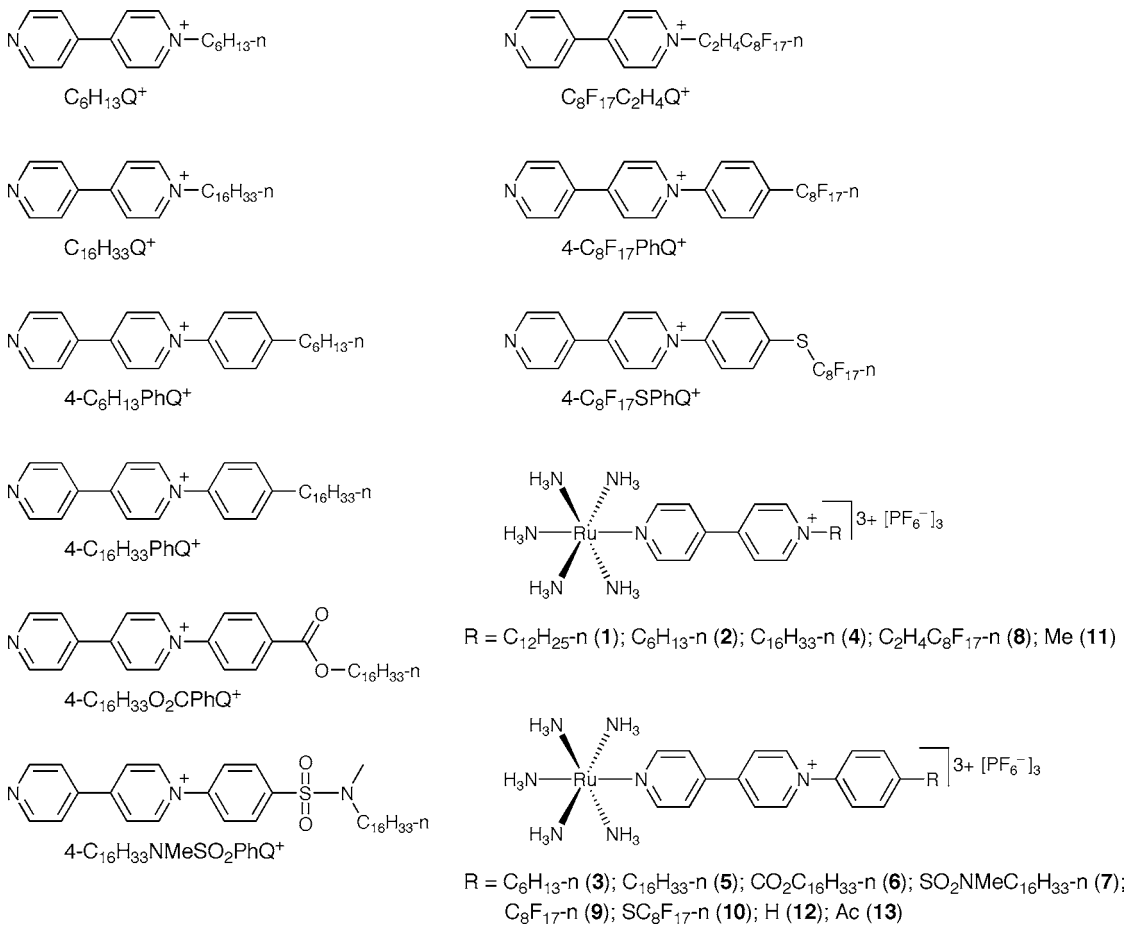

Figure 1. Chemical structures of the proligands and Ru^{II} complex salts investigated, together with the previously reported compound **1**.[11]

precursor salt [2,4-DNPhQ$^+$]BPh_4, together with 1.5 equivalents of an aniline derivative and a small excess of triethylamine. The latter and related aliphatic bases have been shown previously to facilitate the conversion of 5-arylamino-*N*-aryl-2,4-pentadienylideniminium ions (the initial ring-opened products of reacting [2,4-DNPhQ$^+$]Cl with anilines)[24] into *N*-arylpyridinium species.[25] Interestingly, the reactions to produce [4-$C_{16}H_{33}O_2$CPhQ$^+$]PF_6 also afforded as a minor byproduct a material identified as 4,4′-bis(*n*-hexadecyloxycarbonyl)-azobenzene, derived from reductive coupling of 4-(*n*-hexadecyloxycarbonyl)aniline; similar byproducts were detected in the other related syntheses, but not isolated. The syntheses of the proligands used in this work are summarized in Scheme 1.

The *n*-hexyl-substituted complex salts **2** and **3** were synthesized by reacting the appropriate proligand PF_6^- salts with approximately stoichiometric quantities of $[Ru^{II}(NH_3)_5(H_2O)][PF_6]_2$. For all of the other compounds featuring long hydrocarbon or fluorocarbon chains, using the same approach leads to problems relating to the removal of the uncomplexed proligand salts that show solubilities lower than [C_6H_{13}Q$^+$]PF_6 or [4-C_6H_{13}PhQ$^+$]PF_6. Therefore, a modified procedure was adopted, involving about 1.7 equivalents of $[Ru^{II}(NH_3)_5(H_2O)][PF_6]_2$ and a 3-fold extended reaction time. The unreacted Ru^{II} complex precursor is readily removed by thorough washing with water. The desired products, which show no detectable solubility in water, were obtained in very high yields (77−96%), with no further purification required.

Scheme 1. Syntheses of the New Pyridyl Pyridinium Proligands

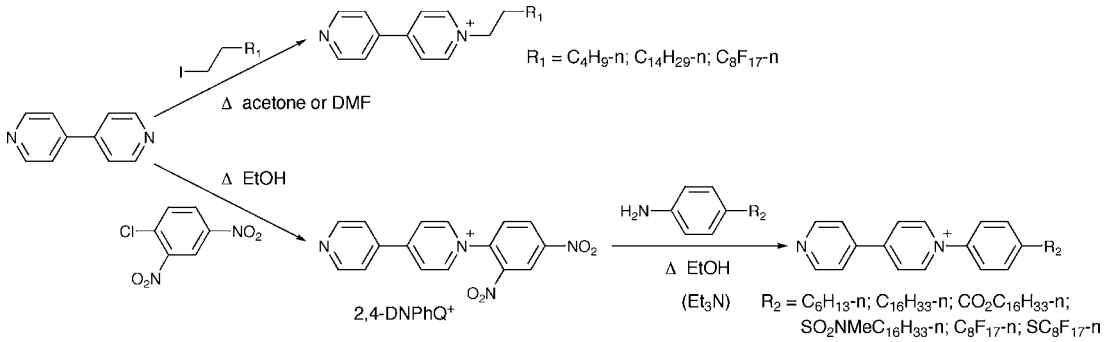

dx.doi.org/10.1021/ic202145b | *Inorg. Chem.* 2011, 50, 12886−12899

Table 2. Selected ^{1}H NMR Data for Complex Salts $[Ru^{II}(NH_3)_5(L^A)][PF_6]_3$[a]

salt (L^A)	pyridyl				R[b]	NH_3	
2 ($C_6H_{13}Q^+$)	9.15		8.70	7.87	4.79	3.52	2.67
3 (4-$C_6H_{13}PhQ^+$)	9.33	9.21	8.85	7.97	7.88	3.61	2.71
4 ($C_{16}H_{33}Q^+$)	9.14–9.22	8.73	7.88	4.79	3.59	2.71	
5 (4-$C_{16}H_{33}PhQ^+$)	9.35	9.22	8.86	7.97	7.88	3.63	2.73
6 (4-$C_{16}H_{33}O_2CPhQ^+$)	9.42	9.23	8.91	7.98	8.37	3.67	2.73
7 (4-$C_{16}H_{33}NMeSO_2PhQ^+$)	9.42	9.23	8.92	7.98	8.25	3.69	2.74
8 ($C_8F_{17}C_2H_4Q^+$)	9.33	9.18	8.79	7.90	5.26	3.59	2.70
9 (4-$C_8F_{17}PhQ^+$)	9.47	9.24	8.93	7.99	8.31	3.68	2.74
10 (4-$C_8F_{17}SPhQ^+$)	9.45	9.23	8.92	7.99	8.19	3.68	2.74
11 (MeQ^+)[c]	9.15	9.04	8.68	7.87	4.53	3.50	2.66
12 (PhQ^+)[c]	9.33	9.21	8.86	ca. 8.0	ca. 8.0	3.60	2.70
13 (4-$AcPhQ^+$)[c]	9.40	9.22	8.89	7.97	8.35	3.64	2.72

[a]Recorded at 500 MHz in $(CD_3)_2CO$; all values given in ppm. [b]Refers to triplet signal for CH_2/singlet signal for Me group or doublet signal for C_6H_4 group adjacent to the quaternized N atom. [c]Data taken from ref 17 (but not previously discussed).

^{1}H NMR Spectroscopy. The ^{1}H NMR spectra of all the new Ru^{II} complex salts **2**–**10** are well-defined when recorded in $(CD_3)_2CO$. Selected data are collected in Table 2. The presence of two partially broadened singlet peaks in the regions about 3.7–3.5 and about 2.7 ppm for the NH_3 ligands confirms the presence of the $\{Ru^{II}(NH_3)_5\}^{2+}$ center in all cases.

The ^{1}H NMR data are informative concerning the electronic properties of the various new L^A ligands. When compared with the *N*-alkyl species **2**, **4**, and **11**, most of the pyridyl signals for **8** show downfield shifts as the electron-withdrawing strength of the pyridinium unit increases because of the presence of a C_8F_{17} substituent. A larger corresponding downfield shift of about 0.5 ppm is observed for the triplet signal attributed to the CH_2 group adjacent to the quaternized N atom, but the NH_3 signals remain unchanged. For the *N*-aryl series, the lowest field pyridyl doublet shifts to higher ppm values as the 4-substituent changes in the order H ≈ C_6H_{13} ≈ $C_{16}H_{33}$ < Ac < $C_{16}H_{33}O_2C$ ≈ $C_{16}H_{33}NMeSO_2$ < $C_8F_{17}S$ < C_8F_{17}. Because this signal shows the largest dependence on R, it is reasonable to assign it as being due to the protons *ortho* to the quaternized nitrogen atom, and the observed trend gives an indication of the relative electron-withdrawing strengths of the different ligands. The total shift in this signal on moving from the previously reported MeQ^+ complex in **11** to **9** is more than 0.3 ppm, while the corresponding difference between **9** and **12** is about 0.14 ppm, indicating a significantly enhanced electron-accepting ability of the new 4-$C_8F_{17}PhQ^+$ ligand. Interestingly, within the *N*-aryl series, the lowest field phenyl doublet which we assign to the two protons adjacent to the quaternized N atom shifts to higher ppm values as the 4-substituent changes in the order C_6H_{13} ≈ $C_{16}H_{33}$ ≈ H < $C_8F_{17}S$ < $C_{16}H_{33}NMeSO_2$ < C_8F_{17} < Ac < $C_{16}H_{33}O_2C$, suggesting a rather different ranking of electron-withdrawing abilities. The pattern of shifting among the other signals is less clear, but the low field NH_3 signal (assigned by integration to the single ligand trans to L^A) is sensitive to the nature of L^A, with a downfield shift of about 0.2 ppm on moving from **11** to **7**. The corresponding shift for the other NH_3 signal located to higher field is smaller (ca. 0.1 ppm).

Electronic Spectroscopy. The electronic absorption spectra of the new complex salts **2**–**10** were recorded in acetonitrile, and the results are presented in Table 3, together with data reported previously for **11**–**13**[17] for comparison purposes. Representative spectra of **4**, **5**, and **7** are shown in Figure 2. As expected, all of the new complexes show intense $d(Ru^{II}) \rightarrow \pi^*(L^A)$ MLCT bands in the visible region, together with UV bands due to intraligand $\pi \rightarrow \pi^*$ excitations.

The MLCT energy decreases (i.e., the band becomes red-shifted) as L^A changes in the order $C_{16}H_{33}Q^+$ ≈ MeQ^+ ≈ $C_6H_{13}Q^+$ > $C_8F_{17}C_2H_4Q^+$ > 4-$C_6H_{13}PhQ^+$ ≈ 4-$C_{16}H_{33}PhQ^+$ > PhQ^+ > 4-$C_{16}H_{33}O_2CPhQ^+$ ≈ 4-$C_8F_{17}SPhQ^+$ ≈ 4-$C_8F_{17}PhQ^+$ ≈ 4-$C_{16}H_{33}NMeSO_2PhQ^+$ > 4-$AcPhQ^+$. Such an ordering is generally indicative of increasing ligand electron acceptor ability, but it is worth noting that for the *N*-aryl species, some clear differences are evident in comparison with the trends observed in the ^{1}H NMR spectra (see above). Extending the *N*-alkyl substituent from Me to C_6H_{13} to $C_{16}H_{33}$ has essentially no effect on the UV–vis spectrum, but the presence of a $C_8F_{17}C_2H_4$ substituent red-shifts the MLCT band (E_{max} decreases by ca. 0.07 eV). The C_8F_{17} group hence exerts a significant electron-withdrawing influence, despite the presence of an intervening saturated ethylene unit. For the *N*-aryl chromophores, the C_6H_{13} and $C_{16}H_{33}$ substituents exert detectable electron-donating effects, while the other groups all increase the overall electron accepting ability of the pyridinium unit to a similar extent. According to the MLCT energies, the $C_{16}H_{33}NMeSO_2$ 4-substituent is a little less strongly electron withdrawing when compared with the previously employed acetyl group, although the NMR chemical shifts indicate that the largest, albeit localized deshielding effects are exerted by the C_8F_{17} (lowest field pyridyl doublet) and $C_{16}H_{33}O_2C$ (lowest field phenyl doublet) substituents (see above).

Electrochemistry. The new complex salts **2**–**10** were studied by cyclic voltammetry in acetonitrile, and the results are presented in Table 3, together with data reported previously for **11**–**13**[17] for comparison purposes. Representative voltammograms of **2** and **3** are shown in Figure 3. All of the new complexes show reversible or quasi-reversible $Ru^{III/II}$ oxidation waves, together with two L^A-based reduction processes. All of these complexes therefore have potential to behave as redox-switchable NLO chromophores,[3a,4] possibly over multiple states. The $Ru^{III/II}$ waves are observed at an almost constant potential (0.44–0.47 V vs Ag–AgCl), showing that the energy of the Ru-based highest occupied molecular orbital (HOMO) is not significantly influenced by changes in the N-substituent.

Although their peak currents are somewhat larger than those of the $Ru^{III/II}$ waves, the reduction events can be assigned to one-electron processes, that is, the stepwise formation of the neutral radical and anionic derivatives of the 4,4′-bipyridinium

dx.doi.org/10.1021/ic202145b | Inorg. Chem. 2011, 50, 12886–12899

Table 3. UV−Vis and Electrochemical Data for Complex Salts $[Ru^{II}(NH_3)_5(L^A)][PF_6]_3$ in Acetonitrile

				$E_{1/2}$, V vs Ag−AgCl (ΔE_p, mV)[b]	
salt (L^A)	λ_{max}, nm[a] (ε, 10^3 M^{-1} cm^{-1})	E_{max} (eV)	assignment	$Ru^{III/II}$	L^A reductions
2 ($C_6H_{13}Q^+$)	591 (15.1)	2.10	d → π*	0.45 (90)	−0.91 (80)
	264 (17.8)	4.70	π → π*		−1.54 (90)
3 (4-$C_6H_{13}PhQ^+$)	623 (19.0)	1.99	d → π*	0.47 (95)	−0.74 (90)
	309 (14.3)	4.01	π → π*		−1.35 (80)
	277 (14.7)	4.48	π → π*		
	257 (14.1)	4.82	π → π*		
4 ($C_{16}H_{33}Q^+$)	589 (15.9)	2.11	d → π*	0.45 (100)	−0.92 (70)
	266 (18.8)	4.66	π → π*		−1.55 (70)
5 (4-$C_{16}H_{33}PhQ^+$)	624 (17.7)	1.99	d → π*	0.47 (90)	−0.72 (95)
	313 (12.4)	3.96	π → π*		−1.33 (90)
	277 (13.1)	4.48	π → π*		
	257 (12.4)	4.82	π → π*		
6 (4-$C_{16}H_{33}O_2CPhQ^+$)	639 (18.5)	1.94	d → π*	0.45 (90)	−0.63 (115)
	284 (22.3)	4.37	π → π*		−1.23 (80)
7 (4-$C_{16}H_{33}NMeSO_2PhQ^+$)	644 (16.2)	1.93	d → π*	0.45 (100)	−0.61 (160)
	280 (18.5)	4.43	π → π*		−1.25 (90)
8 ($C_8F_{17}C_2H_4Q^+$)	610 (17.1)	2.03	d → π*	0.44 (90)	−0.85 (70)
	269 (19.4)	4.61	π → π*		−1.49 (70)
9 (4-$C_8F_{17}PhQ^+$)	642 (19.5)	1.93	d → π*	0.47 (90)	−0.62 (95)
	280 (24.2)	4.43	π → π*		−1.22 (100)
10 (4-$C_8F_{17}SPhQ^+$)	641 (19.6)	1.93	d → π*	0.44 (95)	−0.66 (90)
	284 (22.3)	4.37	π → π*		−1.26 (70)
11 (MeQ^+)[c]	590 (15.8)	2.10	d → π*	0.48 (75)	−0.89 (70)
	268 (16.3)	4.63	π → π*		−1.50 (70)
12 (PhQ^+)[c]	628 (19.3)	1.97	d → π*	0.48 (75)	−0.73 (70)
	286 (20.3)	4.34	π → π*		−1.33 (70)
13 (4-$AcPhQ^+$)[c]	654 (18.0)	1.90	d → π*	0.49 (80)	−0.62 (75)
	270 (25.5)	4.59	π → π*		−1.15 (155)

[a]Solutions ca. 3−8 × 10^{-5} M. [b]Measured in solutions ca. 10^{-3} M in analyte and 0.1 M in $[N(C_4H_9\text{-}n)_4]PF_6$ at a 2 mm disk glassy carbon (**2**−**10**) or Pt (**11**−**13**) working electrode with a scan rate of 200 mV s^{-1}. Ferrocene internal reference $E_{1/2}$ = 0.41 V, ΔE_p = 70 mV. [c]Data taken from ref 17.

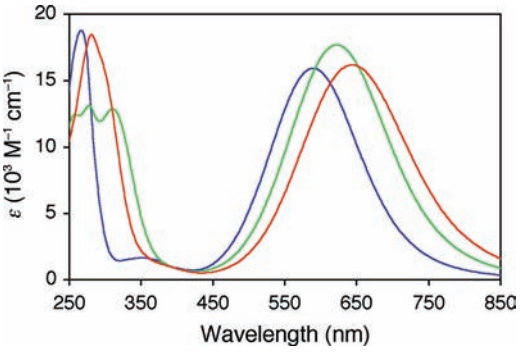

Figure 2. UV−vis absorption spectra of complex salts **4** (blue), **5** (green), and **7** (red) at 293 K in acetonitrile.

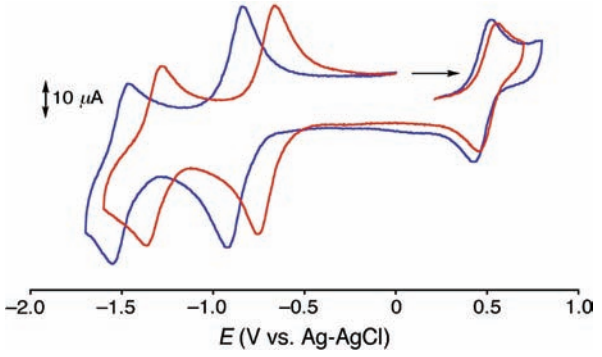

Figure 3. Representative cyclic voltammograms of the complex salts **2** (blue) and **3** (red) with a glassy carbon working electrode in acetonitrile at a scan rate of 200 mV s^{-1} (solutions 10^{-3} M; the arrow indicates the direction of the initial scan).

unit. As with the MLCT energies, the redox potentials reveal the ease of reduction of the various ligands and therefore their overall relative degrees of electron deficiency. The waves for **2** and **4** occur at potentials only slightly lower than those observed for the analogous MeQ^+ complex in **11**. For **8**, significant relative shifts of about +60 mV are observed for both reduction waves, showing that the $C_8F_{17}C_2H_4$ substituent has a detectable stabilizing influence on the LUMO, in keeping with the corresponding MLCT data. The *N*-aryl species show reduction waves at substantially higher potentials still (Figure 3), consistent with their red-shifted MLCT bands and anticipated increased electron-accepting abilities. For these compounds, the first L^A-based reduction process shifts to higher potentials as R changes in the order C_6H_{13} ≈ H ≈ $C_{16}H_{33}$ < $C_8F_{17}S$ < $C_{16}H_{33}O_2C$ ≈ Ac = C_8F_{17} ≈ $C_{16}H_{33}NMeSO_2$, with a total difference between the extremes of 130 mV. For the second L^A-based reduction wave, the trend is C_6H_{13} ≈ H ≈ $C_{16}H_{33}$ < $C_8F_{17}S$ ≈ $C_{16}H_{33}NMeSO_2$ ≈ $C_{16}H_{33}O_2C$ ≈ C_8F_{17} < Ac, with a range of 200 mV. Neither of these orderings corresponds exactly with the trend observed in the MLCT energies, but a broad and logical correlation between the two types of measurement is apparent. In any case, the differences between

dx.doi.org/10.1021/ic202145b | *Inorg. Chem.* 2011, 50, 12886−12899

the E_{max} data and the reduction potentials for the PhQ^+ derivatives with electron-withdrawing 4-substituents do cover only relatively small ranges (ca. 0.04 eV or 50−110 mV), so further comments are probably not justified.

Crystallography. Single crystal X-ray structures were obtained for the proligand salts $[C_6H_{13}Q^+]BPh_4$ and $[C_6H_{13}Q^+]CF_3SO_3$, and also for the complex salt $[Ru^{II}(NH_3)_5(C_{16}H_{33}PhQ^+)]Cl_3\cdot 3.25H_2O$ (**5-Cl**·3.25H_2O). Representations of the molecular structures are shown in Figures 4−6, and selected interatomic distances and angles are

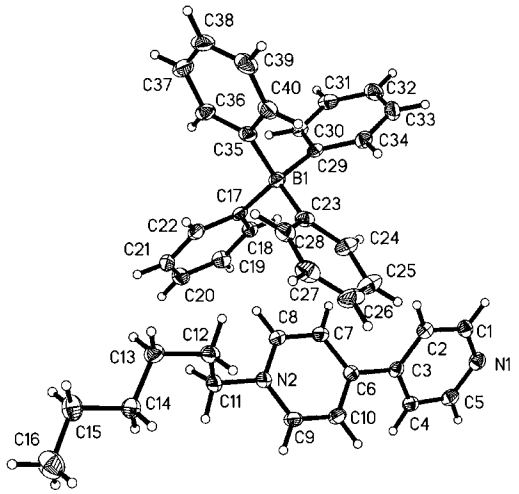

Figure 4. Representation of the molecular structure of the salt $[C_6H_{13}Q^+]BPh_4$, with the disorder in the *n*-hexyl chain removed (50% probability ellipsoids).

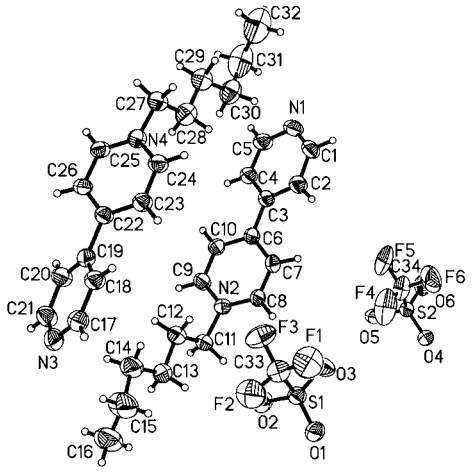

Figure 5. Representation of the molecular structure of the salt $[C_6H_{13}Q^+]CF_3SO_3$ (50% probability ellipsoids).

presented in Tables 4 and 5. A few X-ray structures for compounds containing the $\{Ru^{II}(NH_3)_5\}^{2+}$ moiety coordinated to pyridyl ligands have been reported previously,[27] but the only other one containing a 4,4′-bpy unit is the binuclear complex salt $[Ru^{II}(2,2'\text{-bpy})(tpy)(\mu\text{-}4,4'\text{-bpy})Ru^{II}(NH_3)_5][PF_6]_4\cdot MeCN$ (tpy = 2,2′:6′,2″-terpyridyl).[26b]

The geometric parameters of the 4,4′-bpy fragments in $[C_6H_{13}Q^+]BPh_4$ and $[C_6H_{13}Q^+]CF_3SO_3$ (Table 4) are similar to those observed in the related salt $[MeQ^+]I$.[27] However, the size of the dihedral twist within these units varies greatly over a range of about 13−46°, being 24.21(0.00)° in $[MeQ^+]I$[27] and 30.06(0.13)° in the other independent cation in $[C_6H_{13}Q^+]$-CF_3SO_3.

In cation 1 of **5-Cl**·3.25H_2O, the Ru−NH_3 bond located trans to the 4-$C_{16}H_{33}PhQ^+$ ligand is about 0.04 Å longer than the average of the other four Ru−NH_3 bonds, with the latter covering a narrow range of about 0.01 Å. For the other cation, the corresponding difference is smaller at about 0.02 Å, but the four equatorial Ru−NH_3 distances cover a larger range of about 0.03 Å. The observed relative extensions of the axial Ru−NH_3 bonds can be ascribed to the differing structural trans effects (STEs) of the NH_3 and 4-$C_{16}H_{33}PhQ^+$ ligands;[28] the latter is a reasonably effective π-acceptor and the presence of π-back-bonding causes a weakening and lengthening of the trans Ru−NH_3 bond when compared with the cis ones. It is however noteworthy that the observed STE varies significantly between the two independent cations in **5-Cl**·3.25H_2O; the Ru−NH_3 bond distances may also be influenced by the electronic effects of H-bonding (in this case involving both the Cl^- ions and water molecules) and also other intermolecular interactions. Corresponding STEs of about 0.04 Å have been observed in $[NH_4][Ru^{II}(NH_3)_5(isn)][PF_6]_3$ (isn = pyridyl-coordinated isonicotinamide)[26a] and $[Ru^{II}(NH_3)_5(Mepyz^+)]I_3$ ($Mepyz^+$ = *N*-methylpyrazinium),[29] while the smaller STE of about 0.02 Å found in $[Ru^{II}(NH_3)_5(py)][CF_3SO_3]_2$ (py = pyridine)[26c] may be attributable primarily to the weaker π-acceptor ability of py when compared with related, more strongly electron-accepting ligands. In $[Ru^{II}(2,2'\text{-bpy})(tpy)(\mu\text{-}4,4'\text{-bpy})Ru^{II}(NH_3)_5][PF_6]_4\cdot MeCN$,[26b] an STE of about 0.03 Å is derived when considering the average of the equatorial Ru−NH_3 bond distances, but the latter actually cover an unusually wide range of about 0.07 Å and one of them is the same length as the Ru−NH_3 bond located trans to the bpy bridging ligand. The structure of a related ligand-bridged complex in $[Ru^{II}(2,2'\text{-bpy})_2(\mu\text{-phenCN})$-$Ru^{II}(NH_3)_5][PF_6]_4$ (phenCN = 5-cyano-1,10-phenanthroline) shows an STE of about 0.05 Å due to the N-coordinated nitrile unit, with the equatorial Ru−NH_3 bond distances covering a range of only about 0.02 Å.[30]

The presence of π-back-bonding causes the Ru−N(L^A) distances in **5-Cl**·3.25H_2O to be shorter by as much as about 0.14 Å when compared with the Ru−NH_3 bonds. These Ru−N(L^A) distances are also significantly shorter than the Ru−N(pyridyl) bonds in the previously published related structures which cover a range of about 2.05−2.06 Å;[26] this observation suggests that the 4-$C_{16}H_{33}PhQ^+$ ligand is a slightly stronger π-acceptor when compared with py, isn, or a $\{Ru^{II}(2,2'\text{-bpy})$-$(tpy)(\mu\text{-}4,4'\text{-bpy})\}^{2+}$ fragment. However, considerably shorter Ru−N distances for the nonammine ligand have been reported for $[Ru^{II}(NH_3)_5(Mepyz^+)]I_3$ (1.95(1) Å)[29] and $[Ru^{II}(2,2'\text{-bpy})_2$-$(\mu\text{-phenCN})Ru^{II}(NH_3)_5][PF_6]_4$ (1.932(8) Å),[30] consistent with the expected even stronger π-electron-accepting abilities of $Mepyz^+$ and an organonitrile group. As also observed in related structures,[26,29] the plane of the coordinated pyridyl ring in **5-Cl**·3.25H_2O approximately bisects the equatorial H_3N−Ru−NH_3 angles.

The 4-$C_{16}H_{33}PhQ^+$ ligands in **5-Cl**·3.25H_2O adopt fairly twisted conformations, with dihedral angles of about 18−22° between the planes of the two pyridyl rings and about 34−36° between the planes of the quaternized pyridyl and *N*-phenyl substituent (Table 5). We have found previously corresponding angles of about 3 and 45° for the unsubstituted PhQ^+ ligand in *trans*-$[Ru^{II}(NH_3)_4(PhQ^+)(PTZ)][PF_6]_3\cdot Et_2O$

dx.doi.org/10.1021/ic202145b | *Inorg. Chem.* 2011, 50, 12886−12899

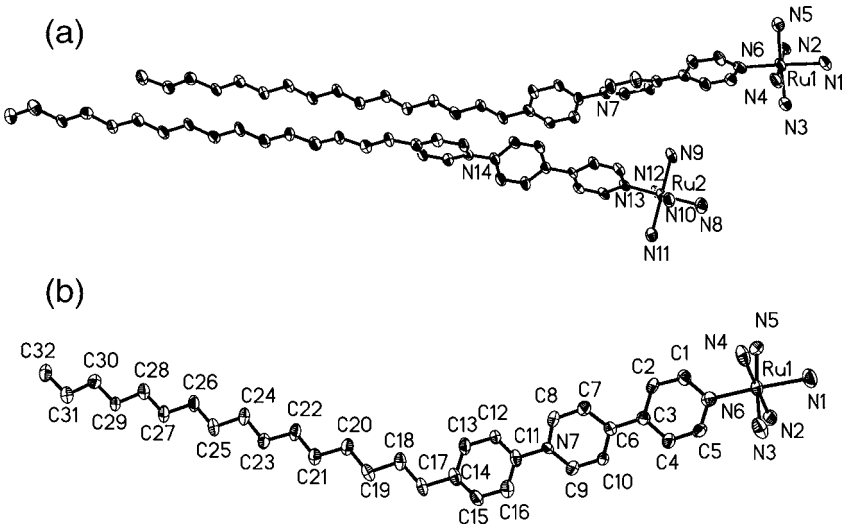

Figure 6. Representations of the molecular structures of the complex cations in the salt **5-Cl**·3.25H_2O, with the water molecules removed for clarity; (a) the two independent cations in the unit cell; (b) alternate view of one of the independent cations (50% probability ellipsoids).

Table 4. Selected Interatomic Distances (Å) and for the Salts $[C_6H_{13}Q^+]BPh_4$ and $[C_6H_{13}Q^+]CF_3SO_3$

	$[C_6H_{13}Q^+]BPh_4$	$[C_6H_{13}Q^+]CF_3SO_3$
C1–N1	1.3381(15)	1.335(5)
C5–N1	1.3365(15)	1.329(5)
C1–C2	1.3826(16)	1.385(5)
C4–C5	1.3833(16)	1.377(5)
C2–C3	1.3893(15)	1.386(5)
C3–C4	1.3900(16)	1.389(5)
C3–C6	1.4796(15)	1.471(5)
C6–C7	1.3947(15)	1.399(5)
C6–C10	1.3922(16)	1.401(5)
C7–C8	1.3659(16)	1.362(5)
C9–C10	1.3689(16)	1.382(5)
C8–N2	1.3467(14)	1.345(5)
C9–N2	1.3478(14)	1.353(5)
C11–N2	1.4826(14)	1.492(4)
dihedral angle[a]	44.89(0.00)	12.81(0.15)

[a]Between the planes of the two pyridyl rings within one 4,4′-bpy unit.

(PTZ = phenothiazine).[17] It should however be noted that structural studies with a series of complex salts containing a *trans*-$\{Ru^{II}Cl(pdma)_2\}^+$ [pdma = 1,2-phenylenebis(dimethylarsine)] center coordinated to related 4,4′-bpy-based ligands show that the intraligand dihedral angles can not be correlated to electronic effects, but rather are determined primarily by crystal packing forces.[31] Comparison of the bond distances for the 4,4′-bpy fragments in **5-Cl**·3.25H_2O with those in $[C_6H_{13}Q^+]BPh_4$ and $[C_6H_{13}Q^+]CF_3SO_3$ shows that coordination to Ru^{II} does not significantly affect the structure of this biaryl unit.

Although the dipoles of the two independent cationic complexes in **5-Cl**·3.25H_2O are approximately aligned (Figure 6a), a network of H-bonds between the Cl^- ions, water molecules, and the H atoms of the NH_3 ligands links the complex units together in an overall centrosymmetric structure which is unfortunately not expected to display significant bulk quadratic NLO effects.

Pressure–Area Isotherms and Langmuir–Blodgett (LB) Film Deposition. Experiments using an ultrapure water subphase and $CHCl_3$ solutions at room temperature showed that of the *n*-$C_{16}H_{33}$-substituted complex salts prepared, only **4** and **5** form stable Langmuir monolayers at the water/air interface, giving well-behaved pressure–area isotherms. The reasons why **6**–**11** failed to produce the desired monolayers are unclear at present, but these observations highlight how seemingly minor structural changes such as including an ester linkage (i.e., on moving from **5** to **6**) can dramatically alter the behavior of such amphiphilic complexes. The isotherm for **5** recorded under a constant compression of 5 mm min^{-1} (Figure 7) shows a steep rise in surface pressure with a high collapse pressure of about 55 mN m^{-1}. Assuming that the layer formed is monomolecular, the limiting surface area per molecule obtained from extrapolation of the steepest portion of the curve to 0 mN m^{-1} pressure is 12 $Å^2$. Considering that the limiting surface area for a linear fatty acid such as arachidic acid is about 20 $Å^2$, the calculated value for complex **5** indicates that the molecules are aggregated or stacked and the film is not a single molecule thick. This observation is strongly reminiscent of studies with a nickel bis(dithiolene) complex.[32] The compression experiment was repeated several times, leading to the same Langmuir curve irrespective of the solution concentration, the volume of solution spread on the surface, and the compression rate. It should be noted that the exact structure within the films is not of prime importance in this work, but what is crucial is that the observation of SHG both from a monolayer and from alternating multilayers (see below) proves that the films must contain a noncentrosymmetric arrangement of the complex chromophores.

Using the Langmuir monolayers of **4** and **5**, experiments were carried out to deposit LB films on both sides of hydrophilic glass slides by vertical dipping with 5×10^{-4} M $CHCl_3$ solutions. In the case of **4**, film transfer was apparently achieved, but the UV–vis spectrum recorded with 3 layers did not show any MLCT band. A possible explanation for this observation may be that the film redissolves in the water upon successive dipping because of very slight solubility of the complex salt. Similar results were obtained with **4** when using hydrophobic substrates. Despite the uncertainty over the nature of the layer at the interface, the deposition behavior of **5** on glass is uniform and reproducible, with transfer ratios close to unity, and up to 18 layers were deposited. The purple

dx.doi.org/10.1021/ic202145b | *Inorg. Chem.* 2011, 50, 12886–12899

Table 5. Selected Interatomic Distances (Å) and Angles (deg) for the Complex Salt 5-Cl·3.25H_2O (Two Independent Cations)[a]

	cation 1	cation 2
Ru–N(L^A)	2.022(9)	2.015(8)
Ru–NH_3(trans-L^A)	2.161(8)	2.141(9)
Ru–NH_3(trans-NH_3)	2.114(9)	2.103(8)
Ru–NH_3(trans-NH_3)	2.116(9)	2.122(9)
Ru–NH_3(trans-NH_3)	2.117(8)	2.126(9)
Ru–NH_3(trans-NH_3)	2.125(9)	2.135(9)
N–C(H)	1.354(13)	1.341(12)
N–C(H)	1.358(13)	1.359(12)
C(H)–C(H)	1.369(14)	1.395(14)
C(H)–C(H)	1.356(14)	1.370(14)
C(H)–C	1.402(14)	1.380(13)
C(H)–C	1.419(14)	1.401(14)
C–C	1.466(13)	1.484(13)
C–C(H)	1.404(14)	1.396(14)
C–C(H)	1.382(13)	1.377(13)
C(H)–C(H)	1.382(14)	1.348(13)
C(H)–C(H)	1.364(13)	1.369(14)
C(H)–N	1.321(13)	1.359(13)
C(H)–N	1.359(12)	1.359(12)
N(L^A)–Ru–N(NH_3)	90.0(3)	94.0(3)
N(L^A)–Ru–N(NH_3)	88.5(3)	89.1(3)
N(L^A)–Ru–N(NH_3)	93.2(3)	91.9(3)
N(L^A)–Ru–N(NH_3)	91.5(3)	88.3(3)
N(L^A)–Ru–N(NH_3)	177.3(4)	176.8(4)
N(ax-NH_3)–Ru–N(eq-NH_3)	87.5(4)	89.1(4)
N(ax-NH_3)–Ru–N(eq-NH_3)	90.6(4)	87.9(4)
N(ax-NH_3)–Ru–N(eq-NH_3)	89.3(3)	89.1(4)
N(ax-NH_3)–Ru–N(eq-NH_3)	89.5(4)	90.8(4)
N(eq-NH_3)–Ru–N(eq-NH_3)	91.9(4)	91.9(4)
N(eq-NH_3)–Ru–N(eq-NH_3)	178.5(4)	178.3(4)
N(eq-NH_3)–Ru–N(eq-NH_3)	89.2(3)	89.2(3)
N(eq-NH_3)–Ru–N(eq-NH_3)	89.6(4)	89.8(4)
N(eq-NH_3)–Ru–N(eq-NH_3)	176.6(3)	176.8(4)
N(eq-NH_3)–Ru–N(eq-NH_3)	89.3(4)	89.1(3)
dihedral angles 1[b]	17.81(0.33)	21.54(0.32)
dihedral angles 2[c]	34.30(0.32)	36.25(0.33)

[a] L^A = 4-$C_6H_{13}PhQ^+$ ligand. ax = axial; eq = equatorial. The bond distances for the 4,4′-bpy fragment are listed in order of increasing separation from the attached Ru center. [b] Between the planes of the two pyridyl rings within L^A. [c] Between the planes of the quaternized pyridyl and *N*-phenyl substituent within L^A.

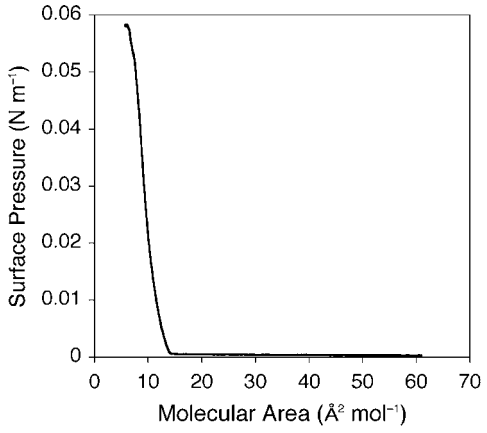

Figure 7. Langmuir Isotherm for **5** at 293 K on a pure water subphase.

coloration of **5** is clearly visible to the naked eye with even a monolayer, and film formation produces a large blue-shift in the MLCT band, with the λ_{max} value becoming 530 nm (corresponding to E_{max} being 0.35 eV higher than that in acetonitrile solution; Table 3). The absorbance at 530 nm increases linearly with the number of layers (*N*, Figure 8),

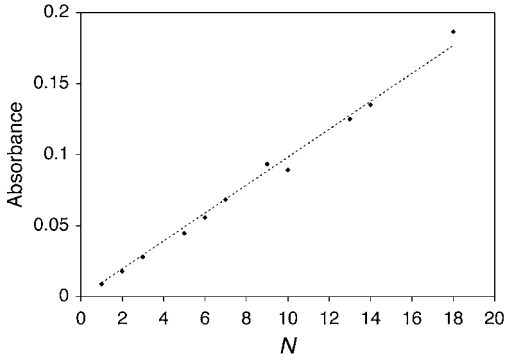

Figure 8. Absorbance at 530 nm of Y-type LB multilayer films of **5** on hydrophilic glass.

consistent with a homogeneous deposition, and is independent of the film thickness. In addition, the films deposited show good stability to air and water. The observed large blue-shift in the MLCT band is indicative of H-aggregates, as observed for example with amphiphilic squaraines which coincidentally show an identical ICT band shift from 630 nm in solution to 530 nm in LB films.[33] In the latter case, the presence of chiral tetramers was invoked,[33,34] although the isotherms recorded did nevertheless afford reasonable molecular areas for the layers formed at the water/air interface.

Perhaps of some relevance, certain UV–vis spectra of **5** recorded in acetonitrile with concentrations above 10^{-5} M show an additional band at about 400 nm, and the intensity of this absorption is strongly concentration dependent. Such an observation, that is unique to **5** of the complex salts studied here, may be indicative of aggregation.

Chemical Redox-Switching of MLCT absorption. Experiments using switching via chemical treatment were carried out by following the approach used in our previous report of solution measurements.[4] Treatment of a Y-type LB multilayer film containing **5** on hydrophilic glass with 30% aq H_2O_2/2 M HCl lead to dissolution of the film because of formation of the highly soluble salt $[Ru^{III}(NH_3)_5(4\text{-}C_{16}H_{33}PhQ^+)]Cl_3$, but using pure H_2O_2 resulted in complete bleaching of the slide. The film was shown to be largely intact by subsequent dipping of the slide into $N_2H_4{\cdot}H_2O$ which restored the color. This redox cycle was repeated four times, yielding two interesting observations: (i) the MLCT band after one cycle is strongly red-shifted to 710 nm and then remains constant; (ii) the absorbance diminishes slowly with repeated cycling. The latter effect is almost certainly attributable to dissolution of the Ru^{III} complex in water, but the cause of the red shift is currently unclear. Similar behavior was noted when using Z-type alternating LB multilayer films containing **5** (see below).

NLO Properties and SHG Studies. HRS studies in acetonitrile gave respective β_0 values of 123, 220, and 354 × 10^{-30} esu for the complex salts **11**, **12**, and **13**.[17] The corresponding values derived from Stark spectroscopic measurements in butyronitrile at 77 K are 120, 186, and 229 × 10^{-30} esu,[35] showing clearly the significant enhancement in

dx.doi.org/10.1021/ic202145b | *Inorg. Chem.* 2011, 50, 12886–12899

quadratic NLO response obtained by replacing the *N*-methyl substituent with a phenyl or 4-acetylphenyl group. Given that the presence of the *n*-$C_{16}H_{33}$ substituent has very little influence upon the MLCT absorption spectrum (or electrochemical behavior), it is hence reasonable to assume that the β_0 response of **5** in solution is about 200×10^{-30} esu, although this can be expected to change significantly in an LB film environment because of local field effects.

Preliminary SHG measurements were carried out with the initially prepared LB films of **5** by using a 1064 nm Nd^{3+}:YAG laser with detection at 45°, and a complete lack of activity confirmed the centrosymmetric Y-type deposition obtained. To produce films capable of showing SHG activity, spacer layers of arachidic acid were also deposited on hydrophilic glass to give alternating noncentrosymmetric multilayered structures, corresponding with a Z-type deposition. Up to 5 bilayers were deposited, once again giving good overall film stability. As with the Y-type films containing **5** alone, these films showed strongly blue-shifted MLCT bands with λ_{max} at 530 nm. To avoid reabsorption of the SHG signal, we attempted SHG studies by using a 1200 nm laser, but this produced only very weak signals. We therefore moved to the 1064 nm fundamental and were then able to observe strong SHG signals, consistent with the bulk polar structure of the alternating films. A periodic fringe pattern was observed with films deposited on both sides of the substrate, so we examined the evolution of the SHG signal using slides with only one coated side. The effects of laser intensity fluctuations were removed by considering the corrected SHG intensity $I_{2\omega}/I_{\omega}^2$ ($I_{2\omega}$ = intensity at 532 nm; I_{ω} = intensity at 1064 nm). As expected, $I_{2\omega}/I_{\omega}^2$ depends quadratically on the number of deposited layers (Figure 9),

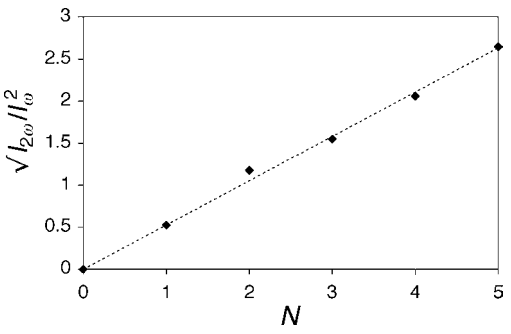

Figure 9. Square root of the corrected SHG intensity at 532 nm of Z-type alternating LB multilayer films containing **5** on hydrophilic glass.

giving additional proof of the homogeneity of the deposition. To carry out redox-switching experiments, an alternating 3 bilayers LB film containing **5** was deposited onto one side of a glass slide coated with ITO and integrated into a custom-built spectroelectrochemical cell.[5g,23] The slide forms the working electrode in the cell and was held at 1 V vs Ag-AgCl for 2 min to oxidize the complex and then at 0 V for 2 min to effect reduction back to the Ru^{II} form. Oxidation causes an about 50% decrease in the SHG intensity, and the signal is almost completely restored following reduction (Figure 10). This process was repeated, giving an essentially reversible switching of the SHG response over 2 cycles, but the response of the Ru^{II} form diminishes with further cycling.

Previous HRS studies showed that the β responses of the model compounds **12** and **13** decrease 10−20-fold upon oxidation and

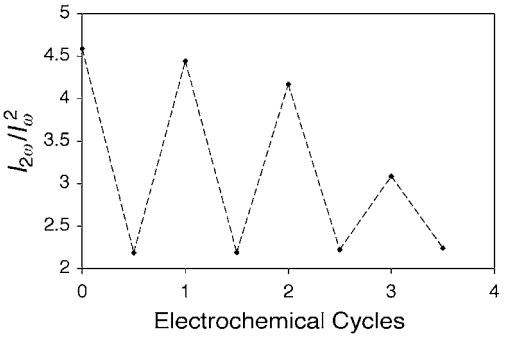

Figure 10. Electrochemical switching of the SHG response at 532 nm of an alternating LB film containing **5** on ITO-coated glass (transmission mode at 45°).

the effect is fully reversible over many cycles.[4] The fact that the SHG from our LB films displays a lower extent of switching may be attributable to several factors. First, the observation of a large blue-shift in the MLCT absorption in the films when compared with acetonitrile solutions is (according to the simple two-state model)[36] indicative of a decreased β_0 response that will lead to a lower SHG activity. Second, almost exact coincidence of the MLCT maximum with the SHG wavelength will lead to reabsorption of some of the SHG by the Ru^{II} form, therefore attenuating the signal detected. Third, the fact that the SHG signal is still substantial after oxidation is indicative of incomplete oxidation arising from the combined effects of the need for charge compensation (oxidation requires BF_4^- ions to migrate from the surrounding electrolyte into the film) and the insulating effects of the long alkyl chains that make up the bulk of the film. The gradual loss of SHG activity for the Ru^{II} form may originate from changes in the film structure, possibly including decomposition due to ligand-loss photochemistry. LB monolayers of **5** give much weaker SHG signals when compared to the alternating multilayers and a convincing redox-switching effect is not observable. It is however possible that the use of more highly active Ru^{II} ammine complex chromophores[7a,b] will allow this phenomenon to be demonstrated using SAMs.

CONCLUSION

We have synthesized and characterized a family of new amphiphilic Ru-based NLO chromophores. Their UV−vis absorption spectra are dominated by intense MLCT bands, the energies of which correlate to some extent with the ligand-based reduction potentials measured by cyclic voltammetry. Single crystal X-ray structures have been determined for two proligand salts and one complex salt, $[Ru^{II}(NH_3)_5(4\text{-}C_{16}H_{33}PhQ^+)]Cl_3 \cdot 3.25H_2O$, revealing centrosymmetric packing structures. The PF_6^- analogue of the latter is the only one of the new complex salts that allows the reproducible deposition of high-quality LB films on glass substrates. Such films on ITO-coated glass show electrochemically induced switching of the SHG response from a 1064 nm laser, with a decrease in activity on oxidation to the Ru^{III} form of about 50%. This effect is reversible, but reproducible over only a few cycles before the signal from the Ru^{II} species diminishes, because of various potential factors such as photochemical degradation. Therefore, we have demonstrated for the first time the redox-switching of bulk NLO activity based on a well-understood molecular-level change. Future studies will use molecular engineering and variations in other aspects such as film thickness, counteranion,

dx.doi.org/10.1021/ic202145b | Inorg. Chem. 2011, 50, 12886–12899

and so forth to increase the magnitude and durability of the effect. Given that MLCT excitation corresponds with internal redox, extrapolation of these studies to include ultrafast photoinduced switching[9b] may also be envisaged.

■ ASSOCIATED CONTENT

Ⓢ Supporting Information

Crystallographic information in CIF format. This material is available free of charge via the Internet at http://pubs.acs.org.

■ AUTHOR INFORMATION

Corresponding Author

*E-mail: b.coe@manchester.ac.uk.

■ ACKNOWLEDGMENTS

We thank the European Commission for a Marie Curie Fellowship (L.B.-L.), the EPSRC (Grant GR/M93864), the Flemish Fund for Scientific Research (FWO-V) for a postdoctoral fellowship (I.A.), the Institute for Promotion of Innovation through Science and Technology in Flanders (IWT-Vlaanderen) for a bursary (S.F.), Leuven University (GOA/2006/03) and the FWO-V (G.0297.04). We are grateful to Dr. Simon P. Foxon for assistance with some of the characterization studies on $[C_6H_{13}Q^+]PF_6$, $[4\text{-}C_6H_{13}PhQ^+]PF_6$, **2** and **3**. Also, we thank Dr. John E. Warren (Synchrotron Radiation Source, CCLRC, Daresbury Laboratory, Warrington, WA4 4AD, U.K.) for assistance with the crystal structure determination of **5-Cl**·3.25H_2O.

■ DEDICATION

This paper is dedicated to Prof Hubert Le Bozec, a pioneer in the field of metal complexes for nonlinear optics, on the occasion of his 60th birthday.

■ REFERENCES

(1) (a) Zyss, J. *Molecular Nonlinear Optics: Materials, Physics and Devices*; Academic Press: Boston, 1994. (b) Bosshard, Ch.; Sutter, K.; Prêtre, Ph.; Hulliger, J.; Flörsheimer, M.; Kaatz, P.; Günter, P. Organic Nonlinear Optical Materials. In *Advances in Nonlinear Optics*; Gordon & Breach: Amsterdam, The Netherlands, 1995; Vol. *1*. (c) *Nonlinear Optics of Organic Molecules and Polymers*; Nalwa, H. S., Miyata, S., Eds.; CRC Press: Boca Raton, FL, 1997. (d) Marder, S. R. *Chem. Commun.* **2006**, 131. (e) *Nonlinear Optical Properties of Matter: From Molecules to Condensed Phases*; Papadopoulos, M. G., Leszczynski, J., Sadlej, A. J., Eds.; Springer: Dordrecht, The Netherlands, 2006.

(2) Recent reviews: (a) Le Bozec, H.; Renouard, T. *Eur. J. Inorg. Chem.* **2000**, 229. (b) Barlow, S.; Marder, S. R. *Chem. Commun.* **2000**, 1555. (c) Lacroix, P. G. *Eur. J. Inorg. Chem.* **2001**, 339. (d) Di Bella, S. *Chem. Soc. Rev.* **2001**, *30*, 355. (e) Goovaerts, E.; Wenseleers, W. E.; Garcia, M. H.; Cross, G. H. In *Handbook of Advanced Electronic and Photonic Materials and Devices*; Nalwa, H. S., Ed.; Academic Press: San Diego, 2001; Vol. *9*, pp 127−191. (f) Coe, B. J. In *Comprehensive Coordination Chemistry II*; McCleverty, J. A., Meyer, T. J., Eds.; Elsevier Pergamon: Oxford, U.K., 2004; Vol. *9*, pp 621−687. (g) Maury, O.; Le Bozec, H. *Acc. Chem. Res.* **2005**, *38*, 691. (h) Cariati, E.; Pizzotti, M.; Roberto, D.; Tessore, F.; Ugo, R. *Coord. Chem. Rev.* **2006**, *250*, 1210. (i) Coe, B. J. *Acc. Chem. Res.* **2006**, *39*, 383. (j) Thompson, M. E.; Djurovich, P. E.; Barlow, S.; Marder, S. In *Comprehensive Organometallic Chemistry III*; Crabtree, R. H., Mingos, D. M. P., Eds.; Elsevier: Oxford, U.K., 2006; Vol. *12*, pp 101−194. (k) Zhang, C.; Song, Y.-L.; Wang, X. *Coord. Chem. Rev.* **2007**, *251*, 111. (l) Andraud, C.; Maury, O. *Eur. J. Inorg. Chem.* **2009**, 4357. (m) Di Bella, S.; Dragonetti, C.; Pizzotti, M.; Roberto, D.; Tessore, F.; Ugo, R. *Top. Organomet. Chem.* **2010**, *28*, 1. (n) Maury, O.; Le Bozec, H. In *Molecular Materials*; Bruce, D. W.; O'Hare, D.; Walton, R. I., Eds.; Wiley: Chichester, U.K., 2010; pp 1−59.

(3) (a) Coe, B. J. *Chem.—Eur. J.* **1999**, *5*, 2464. (b) Asselberghs, I.; Clays, K.; Persoons, A.; Ward, M. D.; McCleverty, J. A. *J. Mater. Chem.* **2004**, *14*, 2831.

(4) Coe, B. J.; Houbrechts, S.; Asselberghs, I.; Persoons, A. *Angew. Chem., Int. Ed.* **1999**, *38*, 366.

(5) (a) Weyland, T.; Ledoux, I.; Brasselet, S.; Zyss, J.; Lapinte, C. *Organometallics* **2000**, *19*, 5235. (b) Malaun, M.; Reeves, Z. R.; Paul, R. L.; Jeffery, J. C.; McCleverty, J. A.; Ward, M. D.; Asselberghs, I.; Clays, K.; Persoons, A. *Chem. Commun.* **2001**, 49. (c) Malaun, M.; Kowallick, R.; McDonagh, A. M.; Marcaccio, M.; Paul, R. L.; Asselberghs, I.; Clays, K.; Persoons, A.; Bildstein, B.; Fiorini, C.; Nunzi, J.-M.; Ward, M. D.; McCleverty, J. A. *J. Chem. Soc., Dalton Trans.* **2001**, 3025. (d) Cifuentes, M. P.; Powell, C. E.; Humphrey, M. G.; Heath, G. A.; Samoc, M.; Luther-Davies, B. J. *Phys. Chem. A* **2001**, *105*, 9625. (e) Paul, F.; Costuas, K.; Ledoux, I.; Deveau, S.; Zyss, J.; Halet, J.-F.; Lapinte, C. *Organometallics* **2002**, *21*, 5229. (f) Powell, C. E.; Cifuentes, M. P.; Morrall, J. P.; Stranger, R.; Humphrey, M. G.; Samoc, M.; Luther-Davies, B.; Heath, G. A. *J. Am. Chem. Soc.* **2003**, *125*, 602. (g) Asselberghs, I.; Clays, K.; Persoons, A.; McDonagh, A. M.; Ward, M. D.; McCleverty, J. A. *Chem. Phys. Lett.* **2003**, *368*, 408. (h) Powell, C. E.; Humphrey, M. G.; Cifuentes, M. P.; Morrall, J. P.; Samoc, M.; Luther-Davies, B. *J. Phys. Chem. A* **2003**, *107*, 11264. (i) Sporer, C.; Ratera, I.; Ruiz-Molina, D.; Zhao, Y.-X.; Vidal-Gancedo, J.; Wurst, K.; Jaitner, P.; Clays, K.; Persoons, A.; Rovira, C.; Veciana, J. *Angew. Chem., Int. Ed.* **2004**, *43*, 5266. (j) Cifuentes, M. P.; Powell, C. E.; Morrall, J. P.; McDonagh, A. M.; Lucas, N. T.; Humphrey, M. G.; Samoc, M.; Houbrechts, S.; Asselberghs, I.; Clays, K.; Persoons, A.; Isoshima, T. *J. Am. Chem. Soc.* **2006**, *128*, 10819. (k) Samoc, M.; Gauthier, N.; Cifuentes, M. P.; Paul, F.; Lapinte, C.; Humphrey, M. G. *Angew. Chem., Int. Ed.* **2006**, *45*, 7376. (l) Dalton, G. T.; Cifuentes, M. P.; Petrie, S.; Stranger, R.; Humphrey, M. G.; Samoc, M. *J. Am. Chem. Soc.* **2007**, *129*, 11882. (m) Wahab, A.; Bhattacharya, M.; Ghosh, S.; Samuelson, A. G.; Das, P. K. *J. Phys. Chem. B* **2008**, *112*, 2842. (n) Guan, W.; Yang, G.-C.; Liu, C.-G.; Song, P.; Fang, L.; Yan, L.; Su, Z.-M. *Inorg. Chem.* **2008**, *47*, 5245.

(6) Kondo, T.; Horiuchi, S.; Yagi, I.; Ye, S.; Uosaki, K. *J. Am. Chem. Soc.* **1999**, *121*, 391.

(7) Selected examples: (a) Coe, B. J.; Jones, L. A.; Harris, J. A.; Sanderson, E. E.; Brunschwig, B. S.; Asselberghs, I.; Clays, K.; Persoons, A. *Dalton Trans.* **2003**, 2335. (b) Coe, B. J.; Jones, L. A.; Harris, J. A.; Brunschwig, B. S.; Asselberghs, I.; Clays, K.; Persoons, A.; Garín, J.; Orduna, J. *J. Am. Chem. Soc.* **2004**, *126*, 3880. (c) Coe, B. J.; Harris, J. A.; Jones, L. A.; Brunschwig, B. S.; Song, K.; Clays, K.; Garín, J.; Orduna, J.; Coles, S. J.; Hursthouse, M. B. *J. Am. Chem. Soc.* **2005**, *127*, 4845. (d) Coe, B. J.; Harries, J. L.; Helliwell, M.; Brunschwig, B. S.; Harris, J. A.; Asselberghs, I.; Hung, S.-T.; Clays, K.; Horton, P. N.; Hursthouse, M. B. *Inorg. Chem.* **2006**, *45*, 1215.

(8) (a) Ulman, A. *An Introduction to Ultrathin Organic Films: From Langmuir-Blodgett to Self-assembly*; Academic Press: Boston, 1991. (b) Petty, M. C. *Langmuir-Blodgett Films: An Introduction*; Cambridge University Press: Cambridge, U.K., 1996. (c) Ashwell, G. J. *J. Mater. Chem.* **1999**, *9*, 1991.

(9) Selected examples: (a) Richardson, T.; Roberts, G. G.; Polywka, M. E. C.; Davies, S. G. *Thin Solid Films* **1988**, *160*, 231. (b) Sakaguchi, H.; Gomez-Jahn, L. A.; Prichard, M.; Penner, T. L.; Whitten, D. G.; Nagamura, T. *J. Phys. Chem.* **1993**, *97*, 1474. (c) Chu, B. W.-K.; Yam, V. W.-W. *Inorg. Chem.* **2001**, *40*, 3324.

(10) (a) Sortino, S.; Petralia, S.; Conoci, S.; Di Bella, S. *J. Am. Chem. Soc.* **2003**, *125*, 1122. (b) Sortino, S.; Di Bella, S.; Conoci, S.; Petralia, S.; Tomasulo, M.; Pacsial, E. J.; Raymo, F. M. *Adv. Mater.* **2005**, *17*, 1390.

(11) Di Bella, S.; Sortino, S.; Conoci, S.; Petralia, S.; Casilli, S.; Valli, L. *Inorg. Chem.* **2004**, *43*, 5368.

(12) Shukla, A. D.; Das, A.; van der Boom, M. E. *Angew. Chem., Int. Ed.* **2005**, *44*, 3237.

(13) Boubekeur-Lecaque, L.; Coe, B. J.; Clays, K.; Foerier, S.; Verbiest, T.; Asselberghs, I. *J. Am. Chem. Soc.* **2008**, *130*, 3286.

(14) Curtis, J. C.; Sullivan, B. P.; Meyer, T. J. *Inorg. Chem.* **1983**, *22*, 224.

(15) (a) Togashi, A.; Matsunaga, Y. *Bull. Chem. Soc. Jpn.* **1987**, *60*, 1171. (b) Adams, R.; Rideal, E. K.; Burnett, W. B.; Jenkins, R. L.; Dreger, E. E. *J. Am. Chem. Soc.* **1926**, *48*, 1758. (c) Tsukinoki, T.; Tsuzuki, H. *Green Chem.* **2001**, *3*, 37.
(16) Hsieh, B. R. *Dyes Pigments* **1990**, *14*, 287.
(17) Coe, B. J.; Harris, J. A.; Harrington, L. J.; Jeffery, J. C.; Rees, L. H.; Houbrechts, S.; Persoons, A. *Inorg. Chem.* **1998**, *37*, 3391.
(18) Matsui, M.; Nakagawa, H.; Joglekar, B.; Shibata, K.; Muramatsu, H.; Abe, Y.; Kaneko, M. *Liq. Cryst.* **1996**, *21*, 669.
(19) *SAINT* (Version 6.45) and *SADABS* (Version 2.10); Bruker AXS Inc.: Madison: WI, 2003.
(20) Sheldrick, G. M. *Acta Crystallogr., Sect. A* **1990**, *46*, 467.
(21) Sheldrick, G. M. *SHELXL 97*, Program for crystal structure refinement; University of Göttingen: Göttingen, Germany, 1997.
(22) *SHELXTL* (Version 6.10); Bruker AXS Inc.: Madison, WI, 2000.
(23) Asselberghs, I.; McDonagh, A.; Ward, M. D.; McCleverty, J.; Coe, B. J.; Persoons, A.; Clays, K. *Proc. SPIE—Int. Soc. Opt. Eng.* **2005**, *5935*, 59350V/1–9.
(24) (a) Zincke, T. *Justus Liebigs Ann. Chem.* **1904**, *330*, 361. (b) Zincke, T.; Heuser, G.; Möller, W. *Justus Liebigs Ann. Chem.* **1904**, *333*, 296.
(25) (a) Marvell, E. N.; Caple, G.; Shahidi, I. *J. Am. Chem. Soc.* **1970**, *92*, 5641. (b) Marvell, E. N.; Shahidi, I. *J. Am. Chem. Soc.* **1970**, *92*, 5646. (c) Kunugi, S.; Okubo, T.; Ise, N. *J. Am. Chem. Soc.* **1976**, *98*, 2282. (d) Eda, E.; Kurth, M. J. *Chem. Commun.* **2001**, 723. (e) Cheng, W.-C.; Kurth, M. J. *Org. Prep. Proced. Int.* **2002**, *34*, 587.
(26) (a) Chou, M. H.; Szalda, D. J.; Creutz, C.; Sutin, N. *Inorg. Chem.* **1994**, *33*, 1674. (b) Szalda, D. J.; Fagalde, F.; Katz, N. E. *Acta Crystallogr., Sect. C* **1996**, *52*, 3013. (c) Shin, Y.-g. K.; Szalda, D. J.; Brunschwig, B. S.; Creutz, C.; Sutin, N. *Inorg. Chem.* **1997**, *36*, 3190.
(27) Coe, B. J.; Foxon, S. P.; Harper, E. C.; Helliwell, M.; Raftery, J.; Swanson, C. A.; Brunschwig, B. S.; Clays, K.; Franz, E.; Garín, J.; Orduna, J.; Horton, P. N.; Hursthouse, M. B. *J. Am. Chem. Soc.* **2010**, *132*, 1706.
(28) Coe, B. J.; Glenwright, S. J. *Coord. Chem. Rev.* **2000**, *203*, 5.
(29) Wishart, J. F.; Bino, A.; Taube, H. *Inorg. Chem.* **1986**, *25*, 3318.
(30) Mellace, M. G.; Fagalde, F.; Katz, N. E.; Crivelli, I. G.; Delgadillo, A.; Leiva, A. M.; Loeb, B.; Garland, M. T.; Baggi, R. *Inorg. Chem.* **2004**, *43*, 1100.
(31) Coe, B. J.; Beyer, T.; Jeffery, J. C.; Coles, S. J.; Gelbrich, T.; Hursthouse, M. B.; Light, M. E. *J. Chem. Soc., Dalton Trans.* **2000**, 797.
(32) Grate, J. W.; Rose-Pehrsson, S.; Barger, W. R. *Langmuir* **1988**, *4*, 1293.
(33) (a) Chen, H.-J.; Law, K.-Y.; Perlstein, J.; Whitten, D. G. *J. Am. Chem. Soc.* **1995**, *117*, 7257. (b) Chen, H.-J.; Law, K.-Y.; Whitten, D. G. *J. Phys. Chem.* **1996**, *100*, 5949.
(34) Chen, H.-J.; Farahat, M. S.; Law, K.-Y.; Whitten, D. G. *J. Am. Chem. Soc.* **1996**, *118*, 2584.
(35) Coe, B. J.; Harris, J. A.; Brunschwig, B. S. *J. Phys. Chem. A* **2002**, *106*, 897.
(36) (a) Oudar, J. L.; Chemla, D. S. *J. Chem. Phys.* **1977**, *66*, 2664. (b) Oudar, J. L. *J. Chem. Phys.* **1977**, *67*, 446.